New Results in Homoheptalene Chemistry

by **Georg Rüedi**[1]) and **Hans-Jürgen Hansen***

Organisch-chemisches Institut der Universität Zürich, Winterthurerstrasse 190, CH-8057 Zürich

The thermal reaction of homoazulene (= bicyclo[5.3.1]undeca-1,3,5,7,9-pentaene; **2**) with dimethyl acetylenedicarboxylate (ADM) in 1,2-dichloroethane ($ClCH_2CH_2Cl$) results, in contrast to an earlier report [5], in formation of not only dimethyl homoheptalene-4,5-dicarboxylate (= bicyclo[5.5.1]trideca-1,3,5,7,9,11-hexaene-4,5-dicarboxylate; **3**), but also of a 4:1 mixture of **3** and dimethyl homoheptalene-2,3-dicarboxylate (**13**) in almost quantitative yield (*Schemes 1* and *3*). The structures of both homoheptalenes have been corroborated by X-ray crystal-structure analysis (*Fig. 5*). The double-bond-shifted (DBS) isomers **3′** and **13′** of **3** and **13**, respectively, could not be detected in their ^{1}H-NMR spectra (600 MHz threshold of detection $\geq 0.5\%$), in agreement with the AM1-calculated ΔH_f° values of the four isomeric homoheptalene-dicarboxylates (*cf. Table 4*). *Vilsmeyer* formylation of homoazulene (**2**) gave homoazulene-8-carbaldehyde (**14**) in a yield of 67%, which, on treatment with benzylidene-(triphenyl)-λ^5-phosphane, gave, in almost quantitative yield, a 1.6:1 mixture of (*Z*)- and (*E*)-8-styrylhomoazulene ((*Z*)-**15** and (*E*)-**15**, resp.). Thermal reaction of the latter mixture with ADM in 1,2-dichloroethane led, in a yield of 42%, to a 5:1 mixture of dimethyl (*Z*)- and (*E*)-2-styrylhomoheptalene-4,5-dicarboxylate ((*Z*)-**15** and (*E*)-**16**, resp.). Both isomers were separated by column chromatography on silica gel. Again, the DBS isomers of (*Z*)-**16** and (*E*)-**16**, *i.e.*, (*Z*)-**16′** and (*E*)-**16′**, could not be detected in the ^{1}H-NMR spectra (600 MHz) of pure (*Z*)-**16** and (*E*)-**16**.

1. Introduction. – The class of homoheptalenes (= bicyclo[5.5.1]trideca-1,3,5,7,9,11-hexaenes) is still sparsely populated, although the parent structure was synthesized more than 25 years ago by *Vogel et al.* [1]. Line-shape analysis of the ^{13}C-NMR signals of homoheptalene (**1a**) in the temperature range of 153–233 K gave an activation energy (E_a) of 5 kcal · mol^{-1} for the double-bond-shift (DBS) process in this [12]annulene, which is slightly higher than that for heptalene itself (3.5 kcal · mol^{-1}), which was derived by the same procedure [2]. Two X-ray crystal-structure analyses of the homoheptalene derivatives **1b** [3] and **1c** [4] have been performed (see below) that show the π-core to be composed of two cycloocta-2,4,6-triene substructures with the 'homo-C(sp^3)-atom' and its two attached C(sp^2)-atoms in common and with a c_2 axis passing through the bridging C-atom (see the AM1-calculated structure of **1a** in *Fig. 1*, which is in good agreement with the X-ray crystal structures of **1b** and **1c** (*Sect. 2.2*). Later, *Scott* and *Kirms* applied *Hafner*'s synthesis of dimethyl heptalene-4,5-dicarboxylates by thermal reaction of azulenes and dimethyl acetylene-dicarboxylate (ADM) (*cf.* [5]) to homoazulene (**2**), for which *Scott et al.* had developed a new and efficient synthesis [6]. They reported that **2** reacts smoothly with ADM in boiling 1,2-dichloroethane ($ClCH_2CH_2Cl$) to yield > 90% dimethyl homoheptalene-4,5-dicarboxylate (**3**)[2]) (*Scheme 1*) [5]. Apart from the specific case of benzo[*b*]homoheptalene [7],

---

[1]) Taken in part from the diploma thesis of *G. R.*, University of Zurich, 2000.

[2]) The locants of homoheptalene (**1a**) are based on the systematic name: tricyclo[5.5.1]trideca-1,3,5,7,9,11-hexaene.

homoheptalene **3** seems, so far, the only known unsymmetrically substituted homoheptalene that, in principle, could exist in two double-bond-shifted (DBS) forms. However, in the ^{1}H-NMR spectrum of **3**, *Scott* and *Kirms* could recognize only the signals that were in agreement with the structure of a 4,5-dicarboxylate.

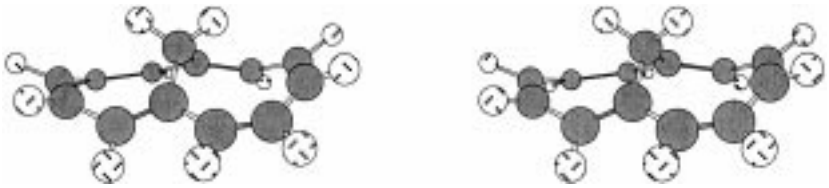

Fig. 1. *AM1-Calculated structure of homoheptalene* (**1a**)

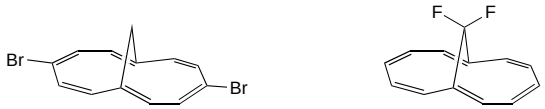

1b **1c**

Scheme 1

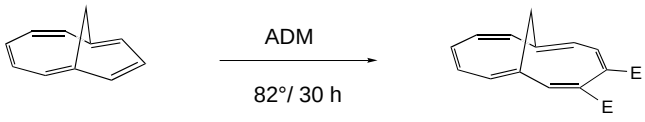

2 **3** (> 90 %)

In the context of our investigations on the DBS isomers of heptalenes as two switchable π-states [8], we also became interested in DBS isomers of unsymmetrically substituted homoheptalenes and decided to repeat the *Scott* and *Kirms*'s synthesis of **3** because we had acquired some skill in the derivatization of heptalene-4,5-dicarboxylates (*cf.* [9]). In the following, we give a first report of our experiments with homoazulene (**2**) and homoheptalene-dicarboxylates derived therefrom.

2. Results and Discussion. – 2.1. *Homoazulene* (**2**). The main steps of the synthesis of homoazulene (**2**) of *Scott et al.* are displayed in *Scheme 2* [6]. The crucial step of the synthesis is based on a catalyzed, intramolecular *Buchner* reaction of the diazo ketone **4**, which is quantitatively available from dihydrocinnamoyl chloride and CH_2N_2[3]). For the formation of 3,4-dihydro-2*H*-azulen-1-one (**5**), we followed an improved procedure of *Scott* and *Sumpter* [10], who obtained **5** as a slightly green oil in 77% yield in boiling CH_2Cl_2 in the presence of catalytic amounts of [$Rh_2(OAc)_4$], ensued by

[3]) We performed all reactions on a larger scale than reported by *Scott et al.* in their synthesis of **2**. This required, at several steps, modifications of the experimental techniques described in the *Exper. Part.*

Scheme 2

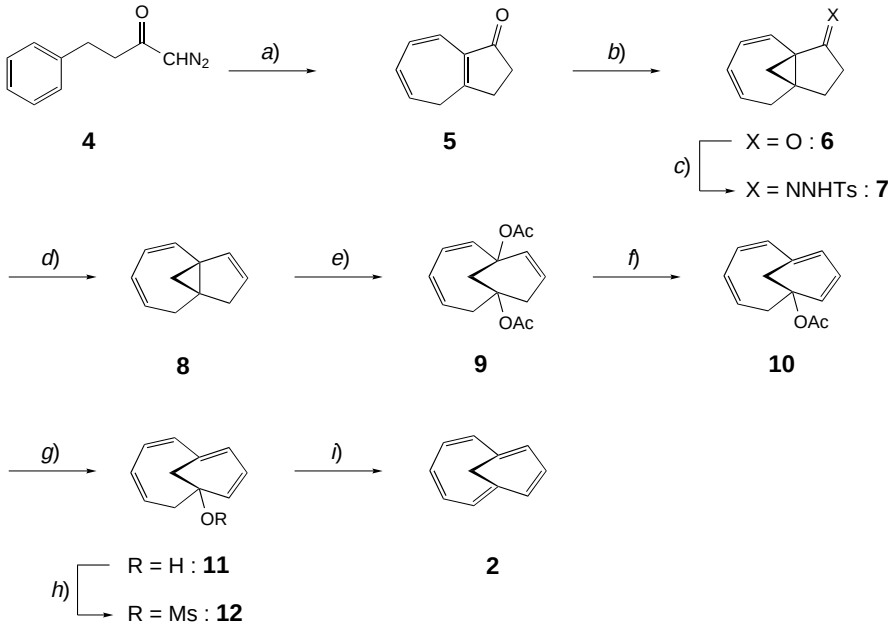

a) $Rh(OAc)_4$, CH_2Cl_2; 61–69%. *b*) $Me_3SO^+I^-$, NaH, DMSO, 75°; 56–62%. *c*) $TsNHNH_2$, THF; 87%. *d*) MeLi, Et_2O; 88–91%. *e*) $Pb(OAc)_4$, benzene, AcOH; 28%. *f*) $Pd(OAc)_2$, Ph_3P, Na_2CO_3, heptane, 85°; 68–96%. *g*) MeLi, Et_2O; 90%. *h*) MsCl, Et_3N, CH_2Cl_2; 97%. *i*) DBN, Et_2O; 50–53%

base-catalyzed DBS. We purified **5** by column chromatography on silica gel and crystallized the material from hexane/*t*-BuOMe 20 : 1. In this way, we obtained pure **5** in yields of 61–69% in colorless crystals (m.p. 29°). The cyclopropanation of **5** with trimethylsulfoxonium iodide in the presence of NaH in dimethyl sulfoxide (DMSO), according to a procedure originally described by *Corey* and *Chaykowsky* [11], led to the tricyclic ketone **6** in yields of 56–62%, which are lower than the yield (76%) reported by *Scott et al.*[4]). The next important step is the *Shapiro* reaction of **7**, the tosyl hydrazone of **6**, with 2 mol-equiv. of MeLi in Et_2O. We obtained the tricyclic triene **8** in yields of 88–91%, which are almost the same as the reported yield of 92%. Nevertheless, we performed our experiments in 10-fold larger runs. The next step, namely the oxidative cleavage of the three-membered ring of **8** by $Pb(AcO)_4$ in benzene in the presence of AcOH to the bicyclic diacetate **9**, was found to be the real obstacle in the synthesis of **2**. *Scott et al.* reported a yield of 73% for this step – a yield that we could neither reach nor approximate, also in applying procedures of other authors (*cf.* [12]). The results of a number of our experiments are collected in *Table 1*.

---

[4]) A control experiment performed exactly under the conditions of *Scott et al.* led also to a yield of 76% of **6**. However, we worked in larger-scale runs with five-fold higher concentrations in DMSO to avoid the use of too-huge quantities of DMSO. Moreover, we reduced the amount of trimethylsulfoxonium iodide applied from 3 to 1.3 mol-equiv. per mol-equiv. of **5**.

Table 1. *Acetoxylation of Tricyclo[5.3.1.0^{1,7}]undeca-2,4,9-triene* (**8**) *with* $Pb(OAc)_4$

$Pb(OAc)_4$	Solvent	Time [h]	Temp. [°]	Yield [%]
1.0 equiv.	Benzene/AcOH 4 : 1	4	25	15
3.0 equiv.	Benzene/AcOH 4 : 1	7	25	17
1.5 equiv.	Benzene	5	25	15
1.5 equiv.	Benzene	5	60	18
1.5 equiv.	AcOH	6	25	20
1.5 equiv.	AcOH	5	100	0
1.5 equiv.	Benzene/AcOH 5 : 2	10	25	23
2.0 equiv.	Benzene/AcOH 5 : 2	9	45	28

The best yield of **9** obtained by us amounted to 28%. Nevertheless, we obtained **9** after chromatography and crystallization from hexane/*t*-BuOMe as colorless crystals, suitable for X-ray crystal-structure analysis (*Fig. 2*), which unambiguously confirmed its structure. The elimination of 1 equiv. of AcOH from **9** with catalytic amounts of $Pd(OAc)_2$ in the presence of Ph_3P and Na_2CO_3 in heptane at 85° caused no specific problems, and acetate **10** was obtained in yields of 68–96%, in agreement with the reported yields of 71–95%. Acetate **10** was obtained as a bright yellow, quite unstable oil, as were the subsequent intermediates **11** and **12**, so that the ensuing steps had to be performed immediately one after the other. In this way, we achieved yields of $\geq$ 90% for each step, in agreement with the yields reported by *Scott et al.* [6]. The latter applied for the last step, the elimination of MsOH from methanesulfonate **12**, *t*-BuOK in *t*-BuOH and finally obtained **2** in a yield of 30%. We found that the elimination reaction with **12** can be performed much more smoothly with a seven-fold excess of 1,5-diazabicyclo[4.3.0]non-5-ene (DBN) in Et_2O at ambient temperature to give pure **2** in yields of 50–53%. *Fig. 3* shows the ^{1}H-NMR spectrum of **2** in (D_6)acetone at 600 MHz with the assignment of all ^{1}H-NMR signals. It is noteworthy that H_a–C(11) exhibits a

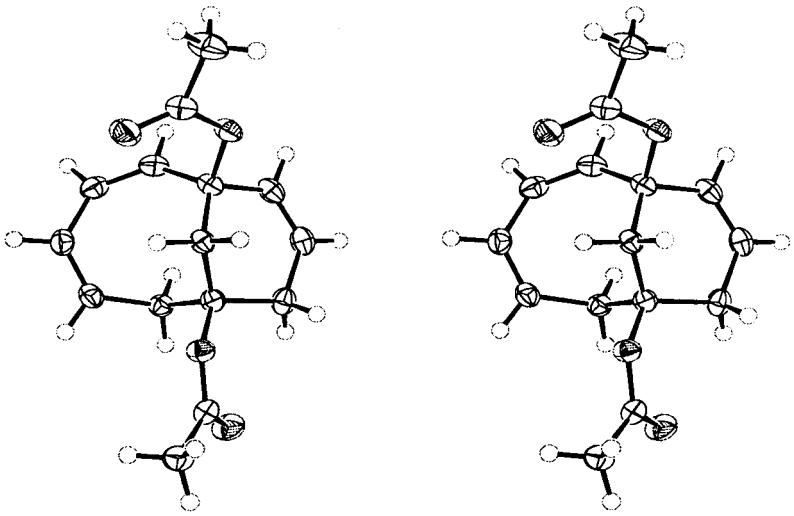

Fig. 2. *Stereoscopic view of the crystal structure of bicyclo[5.3.1]undeca-2,4,9-triene-1,7-diyl diacetate* (**9**)

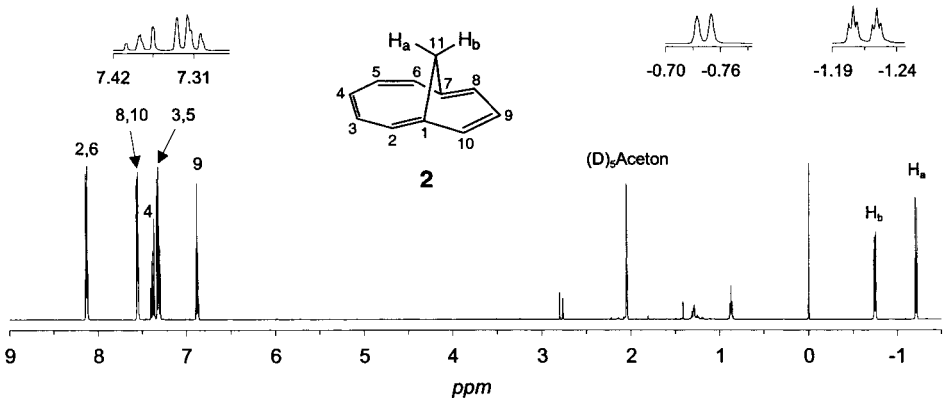

Fig. 3. *^{1}H-NMR Spectrum of homoazulene* (**2**) (600 MHz; (D_6)acetone)

small *W*-like ^4J coupling of 1.6 Hz with H–C(8,10), which is not recognizable for H_b–C(11) and H–C(2,6)[5]).

2.2. *Formation and Structure of Homoheptalenes.* We performed the reaction of **2** with 3-mol-equiv. of ADM in $ClCH_2CH_2Cl$ at 82° as described by *Scott* and *Kirms* [5], monitoring by GC/MS, and were quite excited to find two products in a ratio of 4:1 in the reaction mixture, each with the expected mass of *m*/*z* 284. Our first idea was that the second product may represent the desired DBS isomer of **3**, namely dimethyl homoheptalene-3,4-dicarboxylate (**3′**). After 30 h, the mixture of the two products was collected as a blood-red oil and in a total yield of 96%. The ^{1}H-NMR spectrum ($CDCl_3$) of the mixture indicated, indeed, the presence of two dimethyl homoheptalene-dicarboxylates in a ratio of 4:1, whereby the *s* at 7.19 ppm, attributable to the main isomer, was identical to the reported signal of H–C(6) of **3**. Repeated chromatography of the mixture on a large amount of silica gel with hexane/*t*-BuOMe 4:1 effected enrichment of both compounds, so that further purification was possible by crystallization from hexane/*t*-BuOMe mixtures. The complete analyses of the ^{1}H- and ^{13}C-NMR spectra of both compounds (*cf. Fig. 4* and *Table 2*) revealed that the second homoheptalene derivative, formed in minor amounts, was dimethyl homoheptalene-2,3-dicarboxylate (**13**; *Scheme 3*).

Scott's assignment of the structure of **3** on the basis of its ^{1}H-NMR spectrum at 100 MHz, which did not allow perfect resolution of all ^{1}H signals, could be fully

Scheme 3

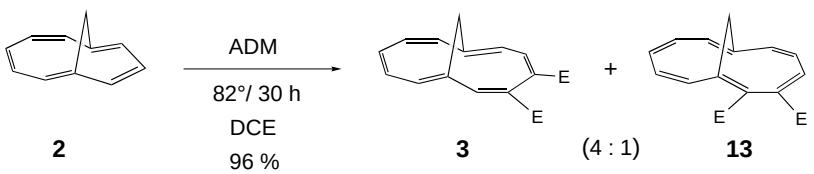

[5]) The locants of **2** are based on its systematic name: bicyclo[5.3.1]undeca-1,3,5,7,9-pentaene.

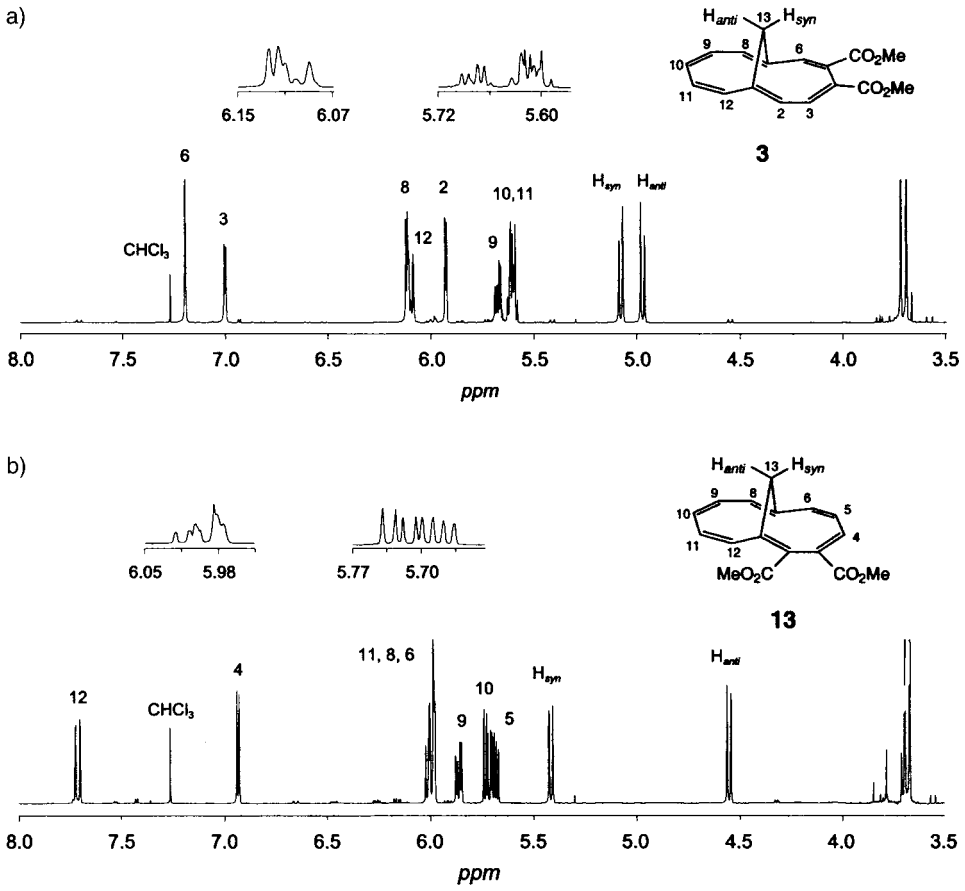

Fig. 4. *^{1}H-NMR Spectra* (600 MHz; $CDCl_3$) *of* a) *dimethyl homoheptalene-4,5-dicarboxylate and* b) *dimethyl homoheptalene-2,3-dicarboxylate* (**3** and **13**, resp.)

Table 2. *^{1}H-NMR Data* (600 MHz, $CDCl_3$) *of the Dimethyl Homoheptalene-dicarboxylates* **3** *and* **13**

Dicarb-oxylate	H–C(2)	H–C(3)	H–C(4)	H–C(5)	H–C(6)	H–C(8)	H–C(9)	H–C(10)	H–C(11)	H–C(12)	H–C(13)
3	5.92 (*d*, *J* = 4.2)	6.99 (*d*, *J* = 4.2)	3.71[a])	3.68[a])	7.19 (*s*)	6.11 (*d*, *J* = 4.7)	5.67 (*dd*, *J* = 11.5, 6.6)	5.60 (*dd*, *J* = 11.5, 6.6)	5.61 (*dd*, *J* = 6.6)	6.09 (*d*, *J* = 12.3)	5.07/4.97 (*J* = 11.3)
13	3.67[a])	3.69[a])	6.93 (*d*, *J* = 6.4)	5.68 (*dd*, *J* = 12.8, 6.4)	5.99 (*d*, *J* = 12.8)	5.99 (*d*, *J* = 5.2)	5.86 (*dd*, *J* = 12.2, 5.2)	5.72 (*dd*, *J* = 12.2, 7.6)	6.00 (*ddd*, *J* = 12.9, 7.6, 0.9)	7.71 (*d*, *J* = 12.9)	5.41 (*dd*, *J* = 11.1, 1.2) 4.55 (*dd*, *J* = 11.1, 0.8)

[a]) *Me*OCO.

confirmed. The appearance of the *s* of H–C(6), already mentioned, as well as the *d* of H–C(3) with $^3J(3,2) = 4.2$ Hz in the low-field region at 7.19 and 6.99 ppm, respectively, is typical for **3**, and allows assignment of the positions of the C=C bonds in this [12]annulene. The chemical-shift difference between H_{syn}–C(13) and H_{anti}–C(13) is with 0.1 ppm quite small, in contrast to **13**, where this difference is 0.86 ppm. Nevertheless, the signal of H_{syn}–C(13), *i.e.*, the H-atom positioned above the E_{Me}-substituted ring, appears in both isomers at lower field. Moreover, a closer inspection of *Fig. 4* reveals that the *AB* systems of CH_2(13) are located almost symmetrically around 5 ppm[6]), or, in other words, the magnitude of the low-field shift of H_{syn} is almost equivalent to that of the high-field shift of H_{anti} with respect to the reference position of 5 ppm for both homoheptalenes. We believe that this observation supports the view that the homotropylium-like structure **13a** contributes to the description of the ground state of **13**, but much less so for **3** and the mesomeric structure **3a**.

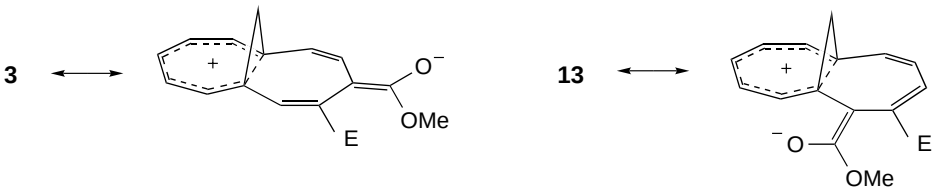

3a **13a**

An observation that confused us at first was the appearance of a comparably low-field *d* at 7.71 ppm, with $^3J = 12.9$ Hz, in the ^{1}H-NMR spectrum of **13**, until we learned from NOESY and COSY experiments that it corresponded to H–C(12). An X-ray crystal-structure analysis of **13** as well as of **3** (*cf. Fig. 5*) showed clearly that, at least in the crystal structure, H–C(12) lies well in the deshielding area of the C=O group of E_{Me}–C(2). Moreover, the crystal-structure conformation represents also the lowest-energy conformation of the AM1-calculated structure of **13**, and it must also be the prevailing conformation, at least in $CDCl_3$ solution, according to the observed chemical shift of the signal of H–C(12).

The most relevant X-ray crystal-structure data of **3** and **13** together with those of the c_2-symmetric homoheptalenes **1b** and **1c** are compiled in *Table 3*. Added to these data are the AM1-calculated structural parameters of the c_2-symmetric parent compound **1a** and, for the purpose of comparison, the X-ray crystal-structure data of dimethyl heptalene-4,5-dicarboxylate (**14**) [13], the homoheptalene counterpart of which is **13**. The average length of the alternating C–C and C=C bonds of the 12e π-perimeter of all structures are, as expected, very close together, and for **13**, one finds almost identical figures as for its heptalene analogue **14**. The slight elongation of d_{av}(C=C) of **14** in comparison with d_{av}(C=C) of **13** is with $< 1\%$ within the limits of the given precisions (see *Table 3*) and, therefore, of no significance. Nevertheless, it shows the expected trend with respect to the distinctly smaller Θ_{av}(C=C–C=C) and Θ_{av}(C–C=C–C) of **14** as compared with those of **13**, which could be ascribed to a

[6]) The centers of the *AB* systems of **3** and **13** are at 5.02 and 4.98 ppm, respectively.

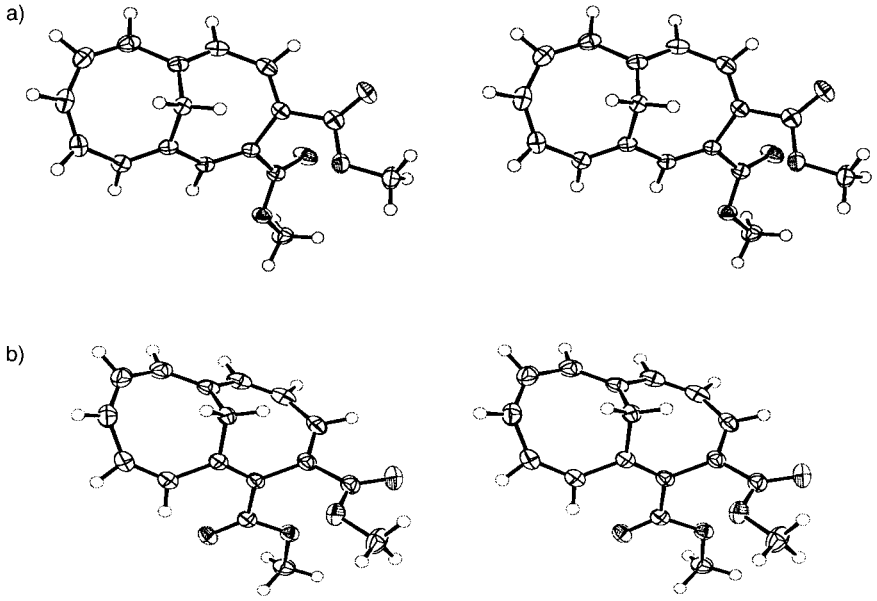

Fig. 5. *Stereoscopic views of the crystal structures of* a) **3** *and* b) **13**

stronger π-interaction in **14**. The higher constraints of the homoheptalene structures are also reflected in their average bond angles (Θ_{av}(C=C−C)), all of which are larger than that of **14**, specifically that of **1c** (+4%), which has almost the same Θ_{av}(C=C−C=C) value as for **14**. On closer inspection of the structural parameters of the homoheptalenes, one recognizes that substituents at the 12e π-perimeter have no significant influence on the corresponding average data. Vicinal substituents as in **3** and **13** may alter the individual parameters of the substructures involved (*cf.*, *e.g.*, the corresponding Θ values of **3** and **13**, which are most susceptible to structural changes); however, these deviations are compensated across the whole molecule due to the structurally imposed constraints of internal motions. The situation changes when a homoheptalene carries substituents at C(13), as is demonstrated by the structural data of **1c** with geminal F-substituents at C(13). Whereas d_{av}(C=C) and d_{av}(C−C) of the perimeter are still comparable with those of the other homoheptalenes, already the ϑ_{av}(C=C−C) value is significantly larger than that of the homoheptalenes that were subjected to X-ray crystal-structure analyses. Responsible for this observation is the steric interaction of the F-substituents with the C(3)=C(4) and C(8)=C(10) bonds, respectively, which reduces the Θ(C(3)−C(4)−C(5)−C(6)) value by $\geq 19°$ as compared with that of the other homoheptalenes. In other words, the F-substituents at C(13) induce flattening of the two π-halves (C(2/8)−C(3/9)−C(4/10)−C(5/11)−C(6/12)) of **1c**, which, in turn, leads to enlargement of the bond angles involved, as expressed as the ϑ_{av}(C=C−C). That this factor reflects a general structural feature and not the consequence of a specific structural behavior of the highly electronegative F-atoms is demonstrated by an AM1 study of 13,13-X_2-substituted homoheptalenes, the most relevant results of which are summarized in *Table 4*. The comparison of the

Table 3. *Comparison of Relevant Structural Data of Homoheptalenes and Dimethyl Heptalene-4,5-dicarboxylate (**14**)*[a])

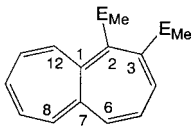

14

Homoheptalene	**1a**[b])	**1b**[c])	**1c**[d])	**3**[e])	**13**[e])	**14**[f])
Interatomic distances *d* [pm]						
C(1)–C(2)	135.0	133.5(3)	135.4(3)	134.9(2)	135.6(2)	138.8
C(1)–C(12)	145.0	145.0(3)	145.8(3)	145.5(2)	145.2(3)	146.8
C(1)–C(13)	149.2	149.6(3)	150.3(2)	151.0(2)	151.3(2)	–
C(2)–C(3)	144.4	145.9(4)	144.9(3)	145.3(2)	149.4(2)	147.5
C(3)–C(4)	134.2	132.2(3)	134.6(3)	133.9(2)	134.1(3)	134.9
C(4)–C(5)	144.3	146.6(3)	144.7(3)	149.8(2)	146.3(3)	142.2
C(5)–C(6)	134.2	133.7(3)	135.6(3)	135.1(2)	134.5(3)	134.5
C(6)–C(7)	145.0	145.0(3)	145.4(3)	145.0(2)	146.5(3)	148.4
C(7)–C(8)	135.0	133.5(3)	135.5(3)	135.1(2)	135.5(3)	137.9
C(7)–C(13)	149.2	149.6(3)	150.3(3)	150.4(2)	150.6(3)	–
C(8)–C(9)	144.4	145.9(3)	145.1(3)	145.8(2)	143.8(3)	144.4
C(9)–C(10)	134.2	132.2(3)	134.2(3)	133.8(2)	135.1(3)	134.0
C(10)–C(11)	144.3	146.6(3)	145.2(3)	147.3(3)	145.7(3)	146.0
C(11)–C(12)	134.2	133.7(3)	134.7(3)	134.7(2)	135.3(3)	136.8
C(1)···C(7)	240.9	241.7	245.0	240.4	238.6	149.3[g])
d_{av} (C–C)	144.6	145.8	145.2	146.5	146.2	145.9
d_{av} (C=C)	134.5	133.1	135.0	134.6	135.0	136.2
Bond angles ϑ [°]						
C(1)–C(2)–C(3)	124.7	125.4	130.2(2)	123.6(2)	121.1(2)	125.4
C(1)–C(13)–C(7)	107.6	107.9	109.2(2)	105.8(1)	104.5(1)	–
C(2)–C(3)–C(4)	129.5	126.1	130.7(2)	128.3(1)	124.2(2)	125.8
C(3)–C(4)–C(5)	131.9	133.0	132.8(2)	127.8(1)	129.0(2)	126.1
C(4)–C(5)–C(6)	133.2	132.7	134.8(2)	131.7(1)	130.8(2)	127.0
C(5)–C(6)–C(7)	130.0	130.9	132.4(2)	130.5(1)	130.6(2)	124.2
C(6)–C(7)–C(8)	120.8	121.1	120.7(2)	120.1(1)	119.0(2)	120.5
C(7)–C(8)–C(9)	124.7	125.4	131.1(2)	124.6(1)	125.8(2)	129.8
C(8)–C(9)–C(10)	129.5	126.1	130.8(2)	128.4(2)	128.5(2)	124.0
C(9)–C(10)–C(11)	131.9	133.0	132.9(2)	131.3(2)	131.7(2)	126.3
C(10)–C(11)–C(12)	133.2	132.7	135.0(2)	134.3(2)	135.7(2)	128.3
C(11)–C(12)–C(1)	130.0	130.9	132.5(2)	129.8(2)	129.6(2)	124.3
C(12)–C(1)–C(2)	120.8	121.1	120.3(2)	121.3(1)	125.2(2)	123.5
ϑ_{av} (C=C–C)	129.9	128.2	130.4	127.6	127.6	125.4
Torsion angles Θ [°]						
C(1)–C(2)–C(3)–C(4)	49.5	47.7	40.1	48.8(2)	67.2(3)	35.7
C(2)–C(3)–C(4)–C(5)	5.2	8.2	2.3	13.9(2)	−0.9(3)	−2.1
C(3)–C(4)–C(5)–C(6)	−37.7	−41.3	−22.0	−48.9(2)	−45.9(3)	−33.1
C(4)–C(5)–C(6)–C(7)	1.7	−2.2	−4.1	−0.7(3)	2.0(4)	2.3
C(5)–C(6)–C(7)–C(8)	163.5	169.6	155.4	170.4(2)	173.9(2)	−132.8
C(6)–C(7)–C(8)–C(9)	179.0	−175.7	−174.5	−175.5(1)	−172.8(2)	−171.2
C(7)–C(8)–C(9)–C(10)	49.5	47.7	40.1	46.9(3)	42.3(3)	28.8
C(8)–C(9)–C(10)–C(11)	5.2	8.2	2.3	7.7(3)	6.9(4)	−0.4
C(9)–C(10)–C(11)–C(12)	−37.7	−41.3	−22.0	−36.0(3)	−30.5(4)	−28.5
C(10)–C(11)–C(12)–C(1)	1.7	−2.2	−4.1	−5.7(3)	−9.7(4)	−3.2
C(11)–C(12)–C(1)–C(2)	163.5	169.6	155.4	170.2(2)	168.5(2)	−134.8
C(12)–C(1)–C(2)–C(3)	179.0	−175.7	−174.5	−175.5(1)	−172.8(2)	−174.3
C(1)–C(2)–C=O	–	–	–	–	−8.5(3)	29.6
C(4)–C(3)–C=O	–	–	–	–	17.8(3)	24.5
C(3)–C(4)–C=O	–	–	–	−21.5(2)	–	–
C(6)–C(5)–C=O	–	–	–	153.1(2)	–	–
Θ_{av} (C=C–C=C)	±43.6	±44.5	±31.1	±45.2	±46.5	±31.5
Θ_{av} (C–C=C–C)	±3.5	±5.2	±3.2	±7.0	±4.9	±2.0

[a]) Torsion angles Θ are given for the (p*R*)-configuration of the homoheptalenes and the (*M*)-configuration of the heptalene **14** (see later in the text). [b]) AM1-Calculated parent structure. [c]) Measurement at ambient temperature; data taken from [3]; e.s.d. for Θ: *ca.* 0.4°. [d]) Measurement at *ca.* 125 K; data taken from [4]; e.s.d. for Θ: *ca.* 0.2–0.5°. [e]) This work; measurements at 173(1) K. [f]) The X-ray crystal-structure data for **14** (dimethyl heptalene-4,5-dicarboxylate) are taken from [13]: e.s.d. values were not available. Locants are chosen according to the systematic name of the underlying parent structure bicyclo[5.5.0]dodeca-1,3,5,7,9,11-hexaene, so that **14** is directly comparable with the homoheptalenes. [g]) It corresponds to the central σ-bond (C(1)–C(7)) in **14**.

calculated and X-ray crystal data of **1c** manifests that the calculations on the 13,13-X_2-homoheptalenes are quite reliable and should closely approximate the actual structures. It is obvious that the increase in bulkiness of the substituents at C(13) leads to a steady augmentation of ϑ_{av}(C=C−C), which is leveled out in the case of **1d** (X = Br) and **1e** (X=Me). These two molecules cannot become flatter in their two π-halves. The five C-atoms of each half involved (see above) lie almost perfectly in a plane (*cf. Table 4*), which also results in nearly identical C−X···C(3/9) and C−X···C(4/10) interatomic distances for **1d** and **1e**. Further steric pressure by substituents at C(13) will push Θ(C(3)−C(4)−C(5)−C(6)), which possesses, for (p*R*)-configured homoheptalenes as well as for (*M*)-heptalenes, normally a negative sign (*cf. Tables 3* and *4*), to positive values as already indicated by the calculated data of (p*R*)-13,13-dimethylhomoheptalene (**1e**) in *Table 4*. This change in the sign of Θ(C(3)−C(4)−C(5)−C(6)) of appropriately 13,13-disubstituted homoheptalenes should have a marked influence on the chiroptical properties of such C_2-symmetric homoheptalenes (see below)[7]).

The UV/VIS spectra of **3** and **13** resemble very much those of comparable heptalenes (see *Figs. 6* and *7* as well as *Table 5*). The homoheptalene absorption band I, which is very broad, appears for both diesters at 420 nm and is directly comparable to the absorption band I of heptalenes (for band definitions, see [8]), which can be recognized, *e.g.*, as a broad band in the spectra of dimethyl 6,8,10-trimethylheptalene-

Table 4. *Comparison of Essential AM1-Calculated Structural Data of 13,13-Disubstituted Homoheptalenes*[a])

Homoheptalene (X)	**1a** (H)	**1c** (F)[b])	**1d** (Br)	**1e** (Me)[c])
Interatomic distances *d* [pm]	134.5	133.1	135.0	134.6
C(13)−X···C(3/9)	255	293 (280)	334	328 (249)
C(13)−X···C(4/10)	258	297 (282)	325	330 (246)
Bond angles ϑ [°]	134.5	133.1	135.0	134.6
C(1)−C(2)−C(3)	124.7	129.2 (130.2)	132.8	133.3
C(2)−C(3)−C(4)	129.5	131.8 (130.7)	135.0	135.6
C(3)−C(4)−C(5)	131.9	133.0 (132.8)	134.8	135.6
C(4)−C(5)−C(6)	133.2	133.2 (134.8)	131.9	131.5
C(5)−C(6)−C(7)	130.0	131.0 (132.4)	127.5	126.8
Torsion angles Θ [°]	134.5	133.1	135.0	134.6
C(1)−C(2)−C(3)−C(4)	49.5	47.7 (40.1)	33.0	26.4
C(3)−C(4)−C(5)−C(6)	−37.7	−21.5 (−22.0)	−0.9	6.5
Deviation of plane [pm][d])	134.5	133.1	135.0	134.6
C(2)−C(3)−C(4)−C(5)−C(6)	11.4	7.5 (7.5)	1.5	1.4

[a]) The torsion angles refer to the (p*R*)-configuration of the homoheptalenes; **1d**: 13,13-dibromo and **1e**: 13,13-dimethyl derivative of **1a**. [b]) In parentheses are the data of the X-ray crystal structure of **1c** at *ca.* 125 K [4]. [c]) C···C Distances are given; in parentheses, distances between closest H-atom of H_3C_{syn}−C(13), and C(3) or C(4). [d]) Least-squares deviation of the plane of the indicated fragment.

---

7) For a hypothetical (p*R*)-13,13-di(*tert*-butyl)homoheptalene, the AM1 calculation indicates that Θ(C(1)−C(2)−C(3)−C(4)) = 11.0° becomes smaller than Θ(C(3)−C(4)−C(5)−C(6)) = 20.4°. These values may be regarded as the lower and upper limits, respectively, of the two Θ of the s-*cis*-butadiene subunits in homoheptalenes, the range of which reaches from 67° (**13**) to 11° and −49° (**3**) to +20°.

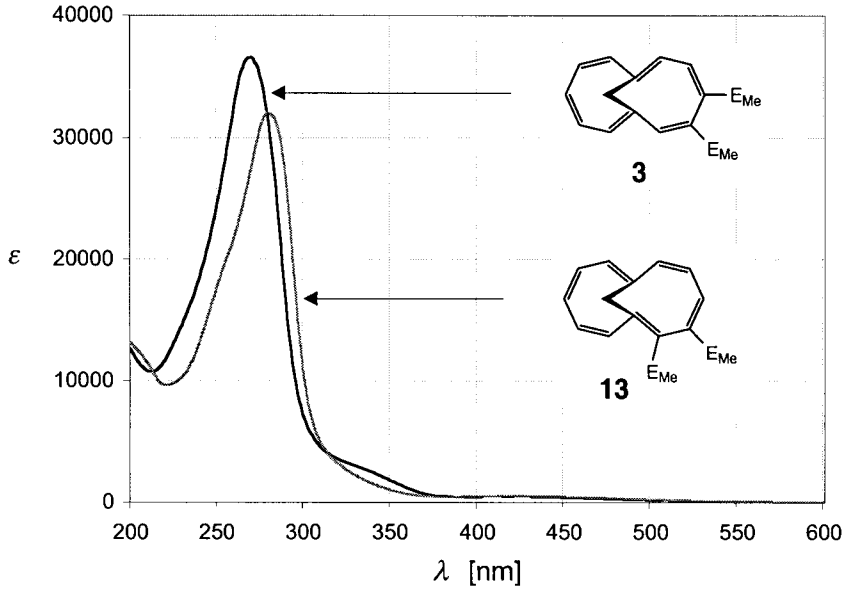

Fig. 6. *UV/VIS Spectra* (hexane) *of* **3** *and* **13**

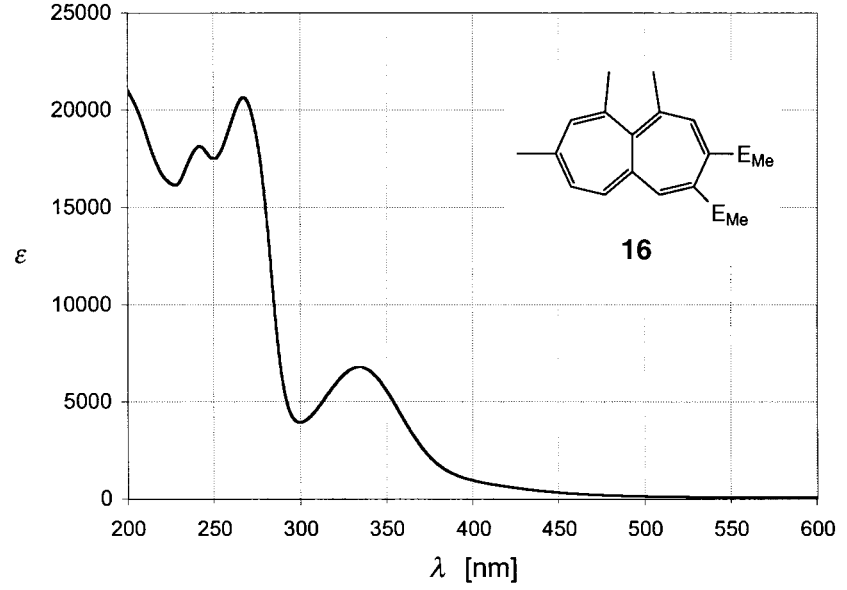

Fig. 7. *UV/VIS Spectrum* (hexane) *of dimethyl 5,6,8-trimethylheptalene-2,3-dicarboxylate* (**16**)

4,5-dicarboxylate (**15**) [8] as heptalene analogue of **13**, or as a broad shoulder in the spectra of dimethyl 5,6,8-trimethylheptalene-2,3-dicarboxylate (**16**) [14] as heptalene analogue of **3**. The homoheptalene absorption band II is visible only as a shoulder at *ca.* 330 nm in the UV/VIS spectrum of **3**, but appears as a clearly separated band at 335 nm

Table 5. *UV/VIS Spectral Data of the Homoheptalene-dicarboxylates* **3** *and* **13**, *and of the Heptalene-2,3-dicarboxylate* **16**

Compound No.	λ_{max} [nm] (ε)		
3	270 (4.50)	330 (sh, 3.65)	419 (2.67)
13	279 (4.51)	–	420 (2.70)
16	242 (4.26)		
	267 (4.31)	334 (3.83)	< 400 (< 2.95)

in **16**. Band II is not clearly recognizable in **13**, but is most certainly buried under the tail of the strong homoheptalene absorption band III at 279 nm. Its heptalene analog **15** shows band II as a shoulder at 328 nm and band III also as a shoulder at 280 nm, followed by a maximum at 261 nm. Bands III appear in **3** (270 nm) and **16** (267 nm) also at similar wavelengths.

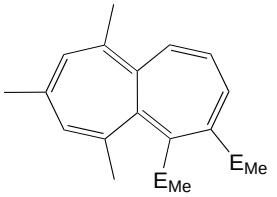

15

In summary, one can state that the UV/VIS absorption behaviors of substituted homoheptalenes and comparable heptalenes are very similar due to the 12e π-perimeters of both structure types. Nevertheless, the inherent chiral topology of both c_2-symmetric π-systems is different, and the methano-bridge of **1a** and its derivatives does not allow ring-inversion processes that lead, in heptalenes, from one enantiomer to the other after double ring-inversion (DRI), principally without involvement of the DBS process (*cf. Scheme 4*). A DBS process in substituted heptalenes occurs at lower temperatures than the DRI process and with retention of a given configuration [15] (see also [16]). In contrast, homoheptalenes change configuration by the DBS process, and the interconversion of one enantiomer into the other is realizable only in symmetrically substituted or at C(4)/C(10)- as well as C(13)-substituted homoheptalenes, since the transition state possesses C_s-symmetry for only these structures (*cf. Scheme 4*).

The X-ray crystal-structure data in *Table 3* demonstrate that the topological differences between homoheptalenes and heptalenes are caused by a change in the sign of Θ at the central s-*trans*-buta-1,3-diene subunits (C(11/5)–C(12/6)–C(1/7)–C(2/8), which is negative for (*M*)-configured heptalenes and positive for (p*R*)-configured homoheptalenes. A comparison of the X-ray values of the torsion angles of **3** and the similarly substituted heptalene-dicarboxylate **16** [14] shows this again quite clearly (*Scheme 5*). Moreover, *Scheme 5* reveals that the (*M*)-topology of heptalenes corresponds with the (p*R*)-topology of homoheptalenes. As a result of this correspondence in the topology of chirality, the *Cotton* effects (CE) and their sign in the long-wavelength region of homoheptalenes and heptalenes with corresponding chiral topologies should be the same. This is indeed the case as confirmed by the CD spectra

Scheme 4

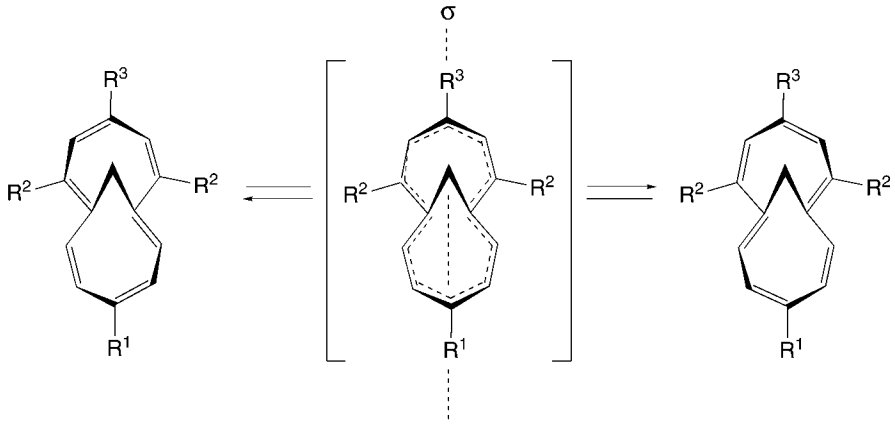

Scheme 5

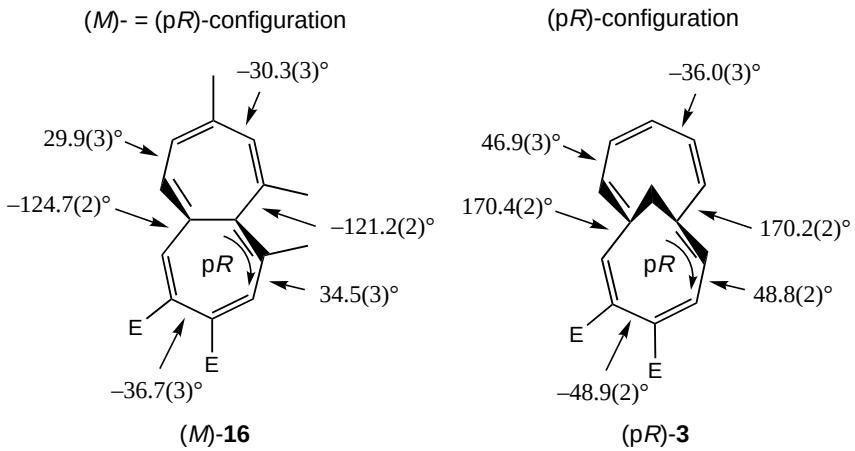

of (p*S*)-**3** and (p*R*)-**3** (*Fig. 8*). The enantiomers of **3** were completely separated on a semipreparative *Chiralcel OD* column (see *Exper. Part*).

Bands I and II of all (*M*)-configured heptalenes exhibit positive CEs, followed by a negative CE for heptalene band III (*cf.* [8][15]). Furthermore, in our hands, all (*M*)-configured heptalene-4,5-dicarboxylates or benzo[*a*]heptalene-6,7-dicarboxylates had distinctly shorter t_R values than their (*P*)-antipodes on *Chiralcel OD* columns with hexane/EtOH or hexane/i-PrOH (*cf.* [16]). Based on these observations, there is little doubt that the enantiomer of **3** with the much shorter t_R value (21 min) and a strong + CE at 425 nm (band I), followed by a second + CE, recognizable as a shoulder at 330 nm (band II), must possess the (p*R*)-configuration (*Scheme 5*). In turn, the (p*S*)-configuration must be ascribed to the enantiomer of **3** with the much larger t_R value (56 min) and the mirror-image CD spectrum (*Fig. 8*). However, the CD spectra of the enantiomers of **3** offer completely independent proof of the absolute configuration of

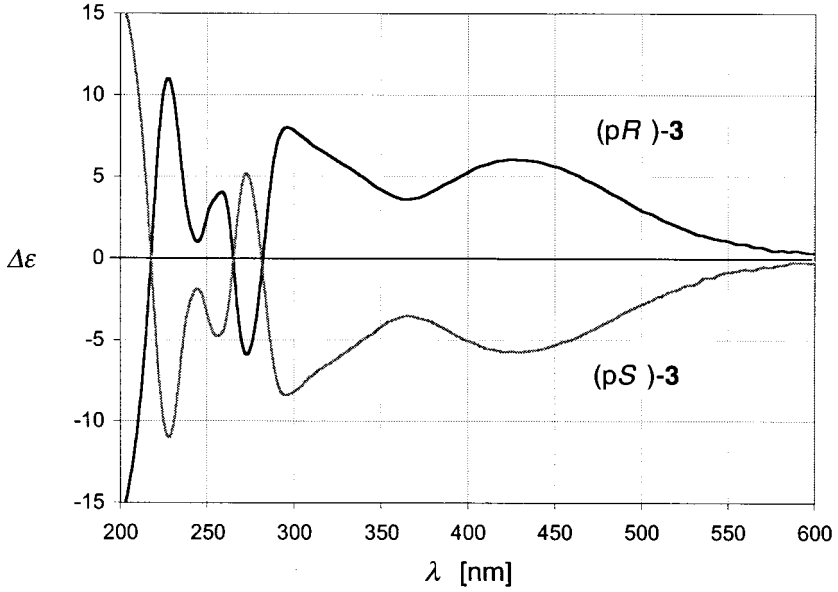

Fig. 8. *CD Spectra* (hexane) *of (p*S*)- and (p*R*)*-**3**

the antipodes. According to the exciton-coupling theory (*cf.* [17]), one expects for the absorption bands of the chirally twisted MeOCO groups a *Davidov* splitting, which should result in opposite signs of their CD in a way that a negative torsion angle between the two groups would cause a negative CE at longer wavelengths, followed a positive CE at shorter wavelengths, and *vice versa* for a positive torsion angle. In other words, for (p*R*)-**3** with a Θ(C(3)–C(4)–C(5)–C(6)) value of – 48.9° (*cf. Scheme 5*; Θ(O=C–C(4)–C(5)–C=O) = – 47.3°), one expects first a negative than a positive CE. Just this situation is met in the CD spectrum of the faster-running antipode of **3**, to which the (p*R*)-configuration has been ascribed according to the above arguments and which exhibits, in the spectral region, where the absorption of α,β-unsaturated ester groups has to be expected, a negative CE at 245 nm and a positive CE at 228 nm.

2.3. *Mechanism of the Homoheptalene Formation.* The thermal reaction of azulenes with ADM, which finally results in the formation of heptalene-4,5-dicarboxylates, leads, in the first step, in a *Diels-Alder*-type addition reaction, to 1,3a-etheno-1,3a-dihydroazulenes of type **18** (*Scheme 6*). These primary intermediates rearrange then *via* zwitterionic intermediates and 1,8a-etheno-1,8a-dihydroazulenes of type **19** into the heptalene-4,5-dicarboxylates (*cf.* [18]). Such a sequence seems to be impossible or at least very unlikely for the thermal reaction of homoazulene (**2**) with ADM due to the energetically unfavorable first step, which, on steric grounds, could not be realized at the *exo*-side of **2**, and it would lead to a highly strained tetracyclic intermediate on the *endo*-side of **2** (*Scheme 6*). This conclusion can be drawn from comparison of ΔH_f° of the AM1-calculated basic structures, derived from the hypothetical reaction of ethyne with azulene (**17**) and with **2**. Moreover, the AM1-calculated ΔH_f° values of all conceivable adducts of ethyne and **2** on the *exo*- and *endo*-side (*Table 6*) reveal that all others are much lower than those of **21** and **22**.

Scheme 6[a])

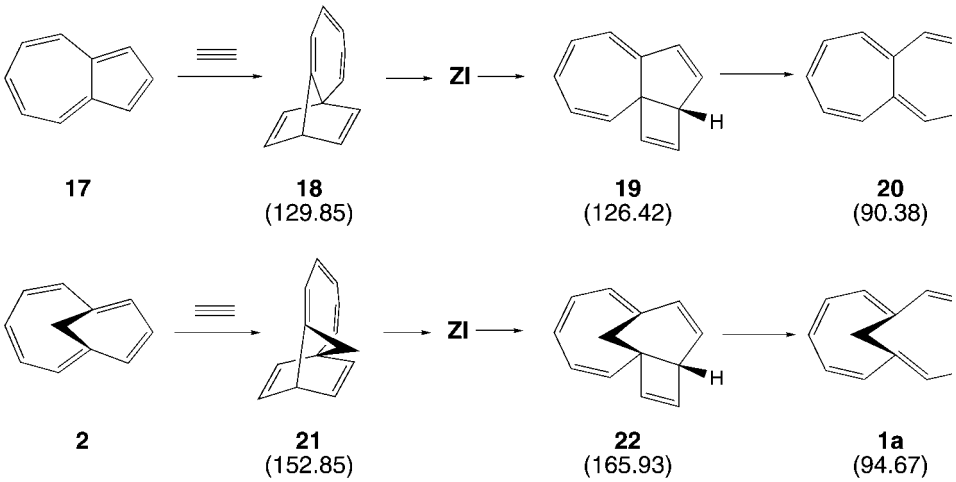

[a]) In parentheses, AM1-calculated ΔH_f° values in kcal · mol^{-1}.

Table 6. *AM1-Calculated* ΔH_f° *Values of Possible Primary* C_2*-Addition Products of Homoazulene* (**2**)[a])

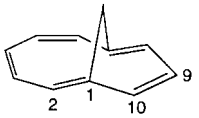

2

C_2-Species Mode of addition	Ethene	TCNE	Ethyne	ADM
exo-10,1	76.59	228.05	123.55	– 38.42
endo-10,1	104.74	255.07	165.93	9.78
exo-10,2	102.85	–[b])	144.47	–[b])
endo-10,2	77.22	232.87	110.84	– 48.84
exo-10,9	80.80	232.65	127.44	– 34.49
endo-10,9	79.74	232.07	126.71	– 35.92

[a]) ΔH_f° in kcal · mol^{-1}. [b]) ΔH_f° not calculated.

Scott and *Kirms* observed that tetracyanoethylene (TCNE; ethane-1,1,2,2-tetracarbonitrile) reacts with **2** already at -45° in THF with formation of solely the *exo*-10,1-adduct (*cf. Table 6*) [5]. Since TCNE reacts with electron-rich π-systems with formation of zwitterions (*cf. e.g.* [19]), they concluded that, under *exo*-attack, TCNE and **2** also form a zwitterion composed of homotropylium and dicyanomethanide parts, which then collapse to the *exo*-10,1-adduct. Indeed, the *exo*-10,1-adduct is, according to AM1 calculations (*Table 6*), by 4.60 kcal · mol^{-1} more stable than the corresponding *exo*-10,9-adduct that could also be formed by collapse of the zwitterions. The formation of an *exo*-adduct from **2** and TCNE is also in agreement with investigations of *Takahashi et al.*, who demonstrated that bicyclo[4.3.1]decatetraenide, an anion that is isoconjugate with **2**, exhibits exclusively *exo*-selectivity on attack of electrophiles such

as deuteron, CO_2 or alkyl and silyl halides [20]. CNDO/2 Calculations of these authors were in agreement with a preferred *exo*-attack of electrophiles due to outward-bent orbital lobes at C(7) and C(9) on the *exo*-face and, in turn, inward-bent orbital lobes on the *endo*-face in the HOMO of the anion, which possesses a nodal plane passing through C(8) and the opposite C(3),C(4) bond, thereby causing less bonding interaction with the LUMO of the electrophiles on its *endo*-face. Therefore, it can be assumed that the same *exo*-selectivity will be exhibited by **2** as has already been proposed by *Scott* and *Kirms* on the basis of their result with **2** and TCNE. This means that the electron-poor ADM should attack **2** also exclusively on the *exo*-side under formation of corresponding zwitterions *exo*-**23** (*Scheme 7*), comprising a homotropylium and an allenolate part. The break-down of these zwitterions will give the two cyclobutene *exo*-10,1- and *exo*-10,9 intermediates *exo*-**24** and *exo*-**25**, respectively, which, upon ring opening, form the observed homoheptalenes **13** and **3** (*Scheme 7*). However, the ratio for **3**/**13** of 4:1 determined is not in agreement with the AM1-calculated ΔH_f° values for *exo*-**24** and *exo*-**25** (*cf. Table 6*), which strongly accounts for the almost exclusive formation of *exo*-**24** and thus **13** ($\Delta\Delta H_f^\circ = -3.93$ kcal · mol^{-1} corresponds to *ca.* 99.6% of **13** and 0.4% of **3** at 82°, assuming $\Delta\Delta S_f^\circ \approx 0$), in analogy to the result of the reaction of **2** and TCNE. This discrepancy confirms that *exo*-**23** does not represent a relaxed zwitterion with internal rotational freedom. We, therefore, assume that the addition of ADM to **2** takes place *via* a charge-compensated transition state, leading to *exo*-**23** in a conformation that kinetically favors the formation of the *exo*-10,9-intermediate **25**, from which the homoheptalene-dicarboxylate **3** is derived. Indeed, when we carried out the reaction of **2** and ADM in boiling MeCN as a stronger solvating, polar solvent, we observed the formation of **3** and **13** in a ratio of 3:2, consistent with a larger internal rotational freedom of *exo*-**23** due to its better stabilization by solvation.

We believe we can exclude the possibility that **2** is subject to an *exo*- and *endo*-attack of ADM, which, in addition to *exo*-**23**, will also give *endo*-**23**. Collapse of *endo*-**23** could lead only to the *endo*-10,9-intermediate **25**, since its *endo*-10,1-counterpart would be extremely strained (*cf.* ΔH_f° in *Table 6*). This means that **3** would mainly arise from the *endo*-attack, and **13** from the *exo*-attack of ADM on **2**. However, the AM1-calculated ΔH_f° values in *Table 6* indicate that, in such a case, there would be an energetically much better path for a collapse of *endo*-**23**, namely to form the tetracyclic *endo*-10,2-product **26**, which is favored over *endo*-**25** by almost 13 kcal · mol^{-1} according to their AM1-calculated ΔH_f° value (*cf. Table 6*)[8].

2.4. *π-Substituted Derivatives of* **3**. On the basis of earlier results on electrophilic substitution reactions of **2** by *Scott et al.* [23], we subjected **2** to the *Vilsmeyer* formylation procedure with *N*,*N*-dimethylformamide (DMF) and $POCl_3$ at 0°. After workup and chromatography on silica gel, the pure carbaldehyde **27** was obtained as an unstable red oil in a yield of 67% (*Scheme 8*). A control reaction with azulene (**17**) under identical conditions gave azulene-1-carbaldehyde in a yield of 96%, which demonstrates that some homoazulene-8-carbaldehyde (**27**) may have been destroyed

---

[8]) The cyclization of *endo*-**23** to *endo*-**26** is completely analogous to the exclusive 1,8-addition of ADM to azulenes under *Lewis* acid catalysis [14] [21] [22], in contrast to the purely thermal reaction that follows the path shown in *Scheme 7*.

Scheme 7

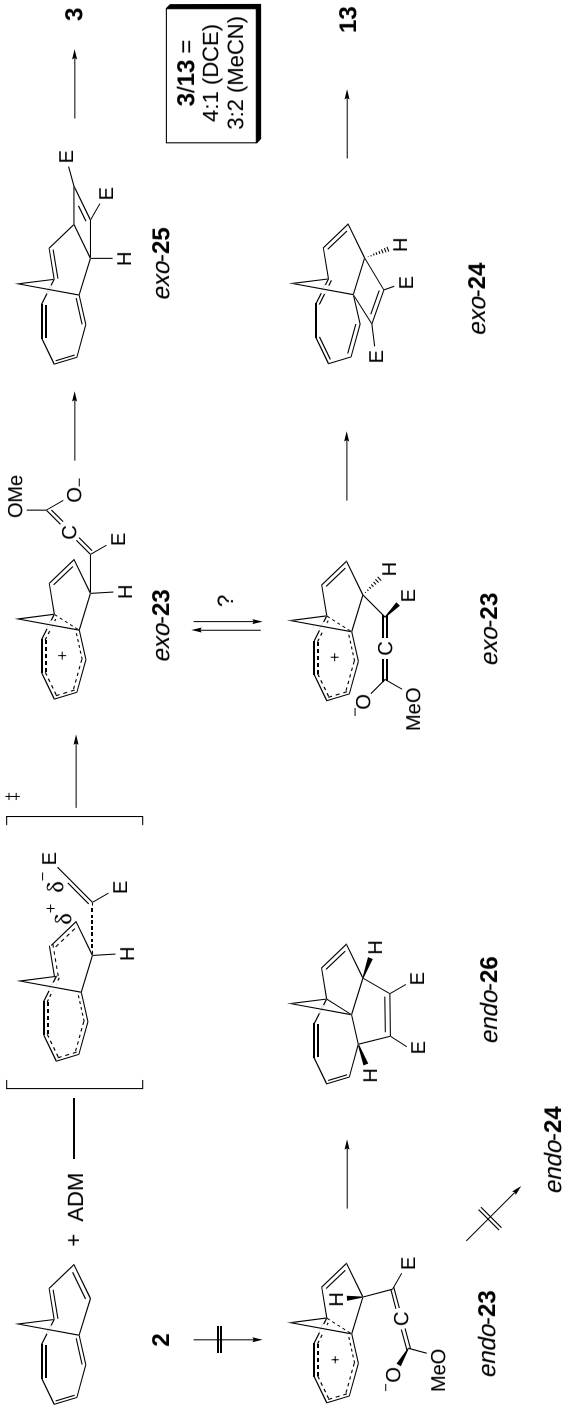
+ ADM
2
endo-23
endo-26
endo-24
exo-23
exo-25
3
3/13 = 4:1 (DCE) 3:2 (MeCN)
exo-23
exo-24
13
MeO
OMe
E
H
?

Scheme 8

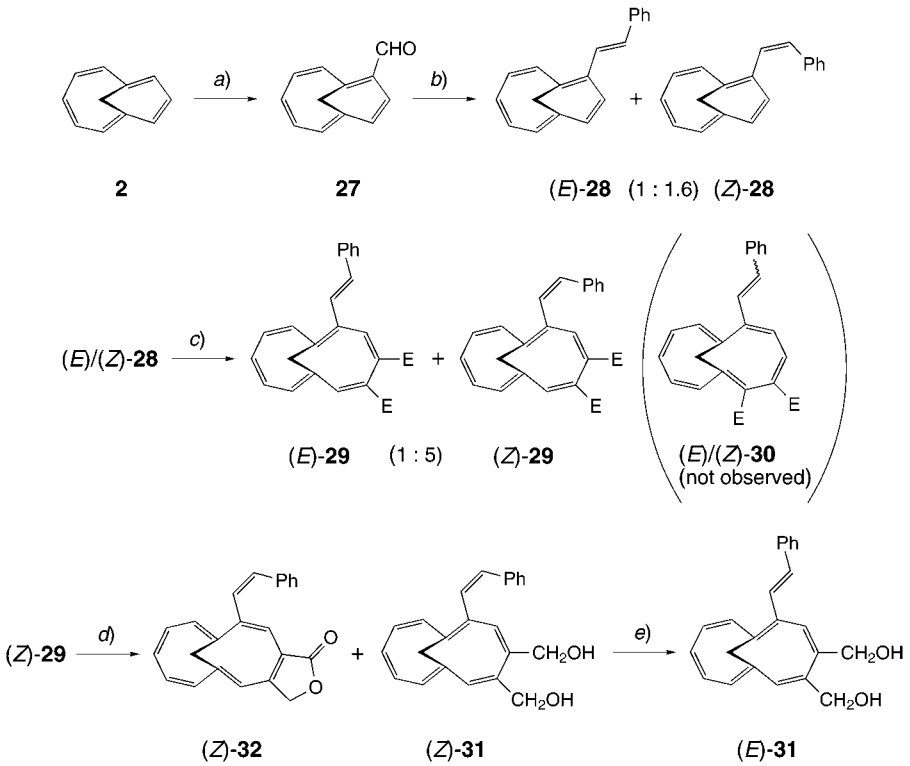

a) 1. $POCl_3$ (1.2 equiv.)/DMF, 0°; 2. 1 equiv. **2** in DMF, 0°/15 min; 67%. *b*) 1. $[Ph_3PCH_2Ph]^+Br^-$ (3.24 equiv.)/*t*-BuOK (3.43 equiv.)/THF, 20° → – 78°. 2. 1 equiv. **15** in THF, – 78°/15 min → 20°/1 h; 99%. *c*) 1 equiv. (*E*)/(*Z*)-**28**/$ClCH_2CH_2Cl$ and 2.64 equiv. ADM, 82°/18 h; 42%. *d*) 1 equiv. (*Z*)-**29**/toluene and 1.8 equiv. of 1.5M DIBAH/toluene, – 90°/4 h; 28% of (*Z*)-**31** and 19% of (*Z*)-**32**. *e*) On standing in an ice-box for 1 h; quantitative.

already during workup and chromatography (*cf.* [23]). Whereas the reduction of the aldehyde function of **27** to a Me group with $NaBH_4/BF_3 \cdot Et_2O$ in diglyme/Et_2O (*cf.* [24]), a procedure that is very successful in the case of azulene-1-carbaldehydes (*cf.*, *e.g.*, [18a][25]), failed since **2** was destroyed under the reaction conditions, we were able to perform a *Wittig* reaction with **2** and benzylidene(triphenyl)λ^5-phosphane in THF at – 78 to 0°. The corresponding 8-styrylhomoheptalene **28** was obtained in almost quantitative yield as a 1.6 : 1 (*Z*)/(*E*)-mixture. The two isomers could be isolated by chromatography on alumina with hexane as eluant as dark red oils, which have been fully characterized spectroscopically (*cf. Exper. Part*). When the 1.6 : 1 mixture (*Z*)/(*E*)-**28** was reacted with ADM in boiling $ClCH_2CH_2Cl$, the 2-styrylhomoheptalene-4,5-dicarboxylate **29** was obtained in 42% yield as a 5 : 1 (*Z*)/(*E*)-mixture. The (*Z*)- and (*E*)-isomers of the corresponding 2,3-dicarboxylate **30** could not be detected in the reaction mixture, but they might have been formed and destroyed under the reaction conditions. The low yield of **29** in comparison to that of the reaction of **2** and ADM,

and the change of the (*Z*)/(*E*) ratio in the course of the reaction reveal that the formation of (*Z*)-**29** and (*E*)-**29** must have been accompanied by partial destruction of the homoazulenes (*Z*)-**28** and (*E*)-**28**. Nevertheless, by careful and repeated chromatography on silica gel of the 5:1 mixture of (*Z*)/(*E*)-**29** could be separated, whereby (*Z*)-**29** was obtained as a brownish red oil and (*E*)-**29** as brown-red needles. The two isomers were fully characterized spectroscopically (*cf. Exper. Part*). Their UV/VIS spectra in hexane are displayed in *Fig. 9*. In comparison with the spectrum of **3** (*Fig. 6*), a bathochromic shift of 30 nm of band I, accompanied by a slight hyperchromism, is observed for both isomers. Band II is completely buried under the bathochromically shifted intense band III of (*E*)-**29**, due to conjugative interaction of the homoheptalene chromophore with the (*E*)-styryl moiety at C(2). However, (*Z*)-**29** displays band II in comparison with **3** as a strongly enhanced shoulder at 310 nm, since band III of (*Z*)-**29**, which appears at 267 nm (270 nm for **3**), is not markedly influenced by conjugation with the (*Z*)-configured styryl residue at C(2). It forms, on steric grounds, with the homoheptalene π-system a torsion angle of 74.2°, whereby the torsion angle within the styryl group is 33.7° (AM1 calculation of the energetically most relaxed conformer). The corresponding AM1 calculations provided, for (*E*)-**29**, torsion angles of 162.8° and −22.8°, respectively.

The reduction of (*Z*)-**29** with DIBAH in toluene gave the corresponding homoheptalene-4,5-dimethanol (*Z*)-**31** together with some of the homoheptalenofuran-1-one (*Z*)-**32** (*Scheme 8*). On standing, (*Z*)-**31** isomerized completely to (*E*)-**31**. Its UV/VIS spectrum in hexane is displayed in *Fig. 10*. The homoheptalene bands I and II are well-recognizable as shoulders at *ca.* 430 and 362 nm with an enhanced intensity of band I in comparison to that of the corresponding dicarboxylate (*E*)-**29**, which

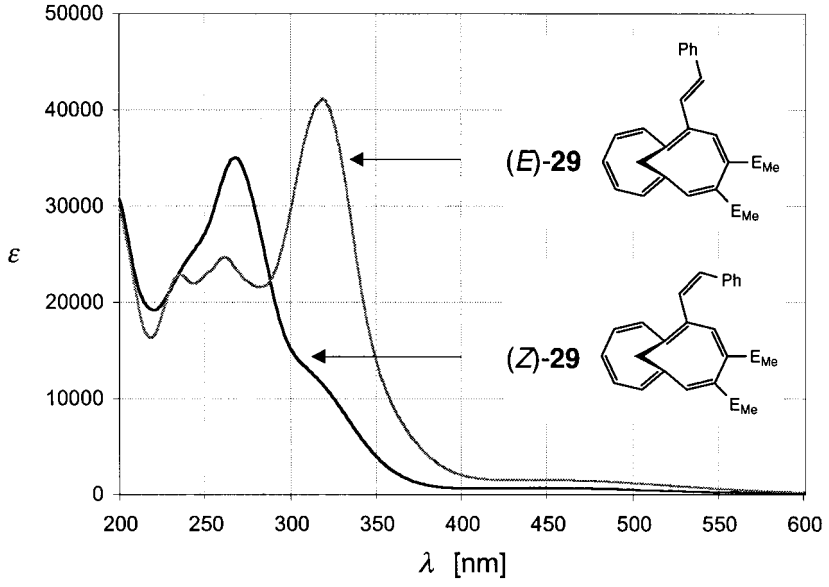

Fig. 9. *UV/VIS Spectra* (hexane) *of dimethyl 1-[(*E*)- and (*Z*)-2-phenylethen-1-yl]homoheptalene-4,5-dicarboxylate* ((*E*) and (*Z*)-**29**)

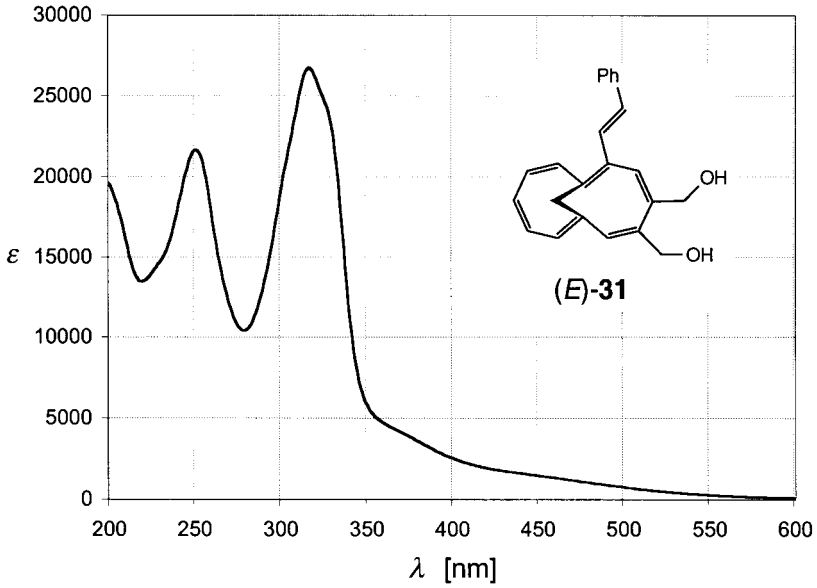

Fig. 10. *UV/VIS Spectrum* (hexane) *of 1-[(*E*)-2-phenylethen-1-yl]homoheptalene-4,5-dimethanol* ((*Z*)-**31**)

appears as a broad maximum at 450 nm (see *Fig. 6*). The absorption band of the (*E*)-styryl-substituted homoheptalene chromophor of (*E*)-**31** and (*E*)-**29** emerges at almost the same wavelength in both compounds, securing the assignment of these bands (see also the UV/VIS spectrum of (*Z*)-**29** in *Fig. 6*, where this band is not present).

Unfortunately, the spectra of none of the new unsymmetrically substituted homoheptanes showed any indication of their DBS isomers. The AM1-calculated ΔH_f° values of the (*E*)- and (*Z*)-isomers of **29**, and their DBS forms **29′** as well as those of the corresponding, but not observed (*E*)- and (*Z*)-isomers of the homoheptalene-2,3-dicarboxylate **30** and their DBS forms **30′** are listed in *Table 7*. In *Table 7* are also included the calculated ΔH_f° values of **3** and **13** and the corresponding Me-substituted dicarboxylates and their DBS forms. All values indicate that the energetically favored

Table 7. *AM1-Calculated* ΔH_f° *Values of the DBS Isomers of Vicinal Dimethyl Homoheptalene-dicarboxylates*[a])

R	H	Me	(*E*)-Styryl	(*Z*)-Styryl
Position of R and E_{Me}				
C(6), C(2,3)	– 64.10	– 69.18	– 22.49	– 19.69
C(2), C(5,6)	– 59.86	– 66.14	– 19.32	– 17.03
$\Delta\Delta H_f^\circ$	– 4.24	– 3.04	– 3.17	– 2.68
C(2), C(4,5)	– 63.92	– 70.34	– 23.58	– 20.30
C(6), C(3,4)	– 62.05	– 67.07	– 20.64	– 17.64
$\Delta\Delta H_f^\circ$	– 1.87	– 3.27	– 2.94	– 2.66

[a]) ΔH_f° in kcal · mol^{-1} for the energetically most relaxed conformers.

DBS forms are those that are comparable with the isolated and characterized isomers **3** and **13** and (*Z*)- and (*E*)-**29**. Therefore, according to AM1 calculations, we had no opportunity to observe their DBS forms in thermal equilibrium. The values also indicate that the C(2)-substituted homoheptalene-dicarboxylates, derived from **3**, exhibit increased $\Delta\Delta H_f^\circ$ values, whereas the C(6)-substituted homoheptalene-dicarboxylates that follow from **13** show slightly decreased $\Delta\Delta H_f^\circ$ values. Both homoheptalene-dicarboxylate series approach, having similar $\Delta\Delta H_f^\circ$ values of *ca.* 3 kcal · mol^{-1} consistent with the 2-methylhomoheptalene being more stable by *ca.* 1 kcal · mol^{-1} than its DBS isomer, 6-methylhomoheptalene, on the basis of AM1 calculations.

We will continue our work with the aim to gain better understanding of the nature of the exited-state of the inherently chiral π-system of the c_2-twisted heptalene and homoheptalene σ-skeletons.

We thank Dr. *A. Linden* for the X-ray crystal-structure determinations, our NMR laboratory, in particular *Nadja Walch*, *Martin Binder*, and Dr. *Gudrun Hopp*, for specific NMR measurements, Prof. *M. Hesse* and his group for mass-spectrometric measurements, and, finally, *Peter Uebelhart* for the chromatographic resolution of the homoheptalene-dicarboxylate. The financial support of this work by the *Swiss National Science Foundation* is gratefully acknowledged.

Experimental Part

General. TLC: glass plates covered with silica gel *60 F_{254}* (*Merck*) or on aluminium foils covered with *Alox 60 F_{254}*, type *E*, 0.2 mm (*Merck*). Column chromatography (CC): silica gel *60* (*Merck*), grain size 0.040–0.063 mm or on alumina (*Fluka*), type *5016 A* basic; act. IV. M.p. (not corrected): *Mettler FP 5/52.* UV/VIS Spectra: were recorded on a *Perkin-Elmer Lambda 19* spectrometer; λ (nm), in parentheses log ε. IR Spectra: *Perkin-Elmer 1600 Series FT-IR* spectrometer; wave numbers in cm^{-1}; characterization of the band intensities (transmission): 0–20% *vs.* 20–40% *s*, 40–60% *m*, 60–80% *w*, 80–100% v*w*. NMR Spectra: *Bruker ARX-300* (300/75 MHz), *Avance DRX-500* (500/125 MHz), and *Avance DRX-600* (600/150 MHz); chemical shifts (δ, ppm) relative to $CD(H)Cl_3$ (7.27/77.00 ppm); for complete assignments of ^{1}H-NMR signals COSY, TOCSY, NOESY, ROESY 2D- or 1D-NMR methods were applied; for complete assignments of ^{13}C-NMR signals HMBC and HSQC 2D-NMR methods were employed. If not stated otherwise, the spectra were recorded at 300 and 75 MHz, resp., in $CDCl_3$. MS: *Varian SSQ 700*; Ionization by EI (70 eV) or Cl (NH_3): *m*/*z*, rel. intensities (%). GC/MS: *Hewlett Packard HP-5971 Series* (mass-selective detector; EI, 70 eV) and *HP-5890 Series II* (GC); carrier gas He; *WCOT* capillary column *HP-5*; 25 m × 0.3 mm, 0.2 μm; injector temp. 280°, starting temp. 100° for 7 min, temp. rate 20°/min, final temp. 240°.

1. Homoazulene and Derivatives. – 1.1. *Bicyclo[5.3.1]undeca-1,3,5,7,9-pentaene* (*Homoazulene*; **2**, *cf.* [2]). 1.1.1. *1-Diazo-4-phenylbutan-2-one* (**4**). In a 2-neck flask I, connected *via* a condenser with a 3-neck flask II, finely powdered KOH (81.0 g, 1.44 mol) was added under ice-cooling to a mixture of carbitol (240 ml), H_2O (120 ml), and Et_2O (80 ml). Flask II contained a soln. of dihydrocinnamoyl chloride (*Fluka*; 71.62 g, 0.425 mol) in Et_2O (100 ml), which was kept by cooling at −10°. Flask I was heated to 55° and, after most of the Et_2O had been distilled into flask II, a soln. of 'diazald' (*N*-methyl-*N*-nitroso-*p*-toluene sulfonamide, *Fluka*; 270.0 g, 1.26 mol) in a mixture of Et_2O (500 ml) and THF (250 ml) was dropped into the mixture of flask I within 2 h, whereby the temp. was maintained at 55°, so that the formed CH_2N_2 was continuously co-distilled with Et_2O into flask II. After all of the soln. of 'diazald' had been added to flask I, Et_2O (50 ml) was added to flask I and distilled into flask II until the distilling Et_2O became colorless. Flask II was brought within 2 h at r.t. and then heated for an additional h at 50°. The excess CH_2N_2 in flask II that distilled off with Et_2O was destroyed by reaction with AcOH. The residual oil was diluted with toluene (*ca.* 50 ml), which was again distilled off. The residue was then completely freed under h.v. from traces of solvents to give **4** (74.04 g, 100%) as a yellow oil. A sample for analysis was purified by CC (silica gel; hexane/Et_2O 1:1). R_f (hexane/Et_2O 1:2) 0.28. UV (hexane): λ_{max} 246 (4.12); λ_{min} 222 (3.60). IR (film): 2105v*s* (CHN_2), 1640v*s* (C=O). ^{1}H-NMR: 7.28, 7.19 (5 arom. H); 5.17 (*s*, H–C(1)); 2.95 (*t*, *J* = 7.7, CH_2(4)); 2.63 (br. *t*, *J* = 7.4, CH_2(3)). ^{13}C-NMR: 193.76 (*s*, C(2)); 140.53 (*s*, C(1) of

Ph); 128.43, 128.21 (2*d*, C_o and C_m of Ph)); 126.15 (*d*, C_p of Ph); 54.45 (*t*, C(4)); 42.26 (*t*, C(3)); 30.82 (*d*, C(1)). GC/MS ($C_{10}H_{10}N_2O$; 174.20): 201 (36), 173 (6, $[M-1]^+$), 146 (13, $[M-N_2]^{+\cdot}$), 118 (15), 115 (8), 91 (56), 65 (14), 55 (100).

1.1.2. *3,4-Dihydro-2*H*-azulen-1-one* (**5**). In a 750-ml 3-neck flask, equipped with an efficient condenser, thermometer, and N_2 inlet, $Rh_2(AcO)_4$ (0.052 g, 0.12 mmol) was dissolved in CH_2Cl_2 (430 ml). The blue-green soln. was heated at reflux (42°), and, under N_2, a soln. of **4** in CH_2Cl_2 (10 ml) was added within 15 h *via* a syringe, driven by a dosage pump, whereby the tip of the elongated hollow needle was placed in the refluxing solvent stream at the condenser. As a result of the very slow addition of **4** and the additional dilution by the refluxing solvent, an optimally high dilution effect for the catalyzed intramolecular *Buchner* reaction could be attained. After the addition of **4**, the soln. was heated for a further h and then cooled to r.t. A small amount of Et_3N (0.2 ml) was added, which caused a transitory darkening from yellow to brown and a spontaneous warming of the soln. to 40°. Finally, the initial yellow color returned. After 0.5 h, the soln. was filtered over silica gel, CH_2Cl_2 was distilled off, and the yellow residue was subjected to CC (silica gel; hexane/*t*-BuOMe 5:1). The slightly greenish yellow oil obtained was crystallized from hexane/*t*-BuOMe/20:1 to give pure **5** (21.87 g, 69%). Colorless needles. M.p. 29°. R_f(hexane/*t*-BuOMe 1:1) 0.29. UV/VIS (hexane): λ_{max} 226 (4.14),267 (3.54); λ_{min} 247 (3.37). IR (film): 3378v*w*, 3023v*s*, 2958*s*, 2922*s*, 2864*m*, 2829*s*, 1695v*s*, 1622v*s*, 1561*m*, 1430v*s*, 1406*s*, 1384*s*, 1334v*s*, 1276v*s*, 1216*m*, 1140v*s*, 1078*m*, 1005*s*, 988*s*, 897*w*, 822*s*, 794*s*, 737v*s*, 697*s*, 660*s*, 622v*s*, 520*m*. ^{1}H-NMR: 6.75 (*d*, $^3J(8,7)=11.1$, H–C(8)); 6.53 (*dd*, $^3J(7,8)=11.1$, $^3J(7,6)=5.8$, H–C(7)); 6.15 (*dd*, $^3J(6,5)=9.9$, $^3J(6,7)=5.8$, H–C(6)); 3.34 (*dt*, $^3J(5,6)=9.9$, $^3J(5,4)=6.3$, H–C(5)); 2.85 (*d*, $^3J(4,5)=6.3$, CH_2(4)); 2.72 (*t*-like, $^3J(2,3)=4.4$, CH_2(2)); 2.52 (m_c, CH_2(3)). ^{13}C-NMR: 205.43 (*s*, C(1)); 165.88 (*s*, C(3a)); 136.98 (*s*, C(7a)); 130.67, 128.62, 122.44, 120.99 (4*d*, C(5,6,7,8)); 35.62 (*t*, C(2)); 31.12 (*t*, C(4)); 29.77 (*t*, C(3)). GC/MS ($C_{10}H_{10}O$; 146.19): 146 (64, $M^{+\cdot}$), 131 (5), 117 (69), 115 (53), 104 (100), 91 (20), 78 (16), 63 (31).

1.1.3. *Tricyclo[5.3.1.0^{1,7}]undeca-2,4-dien-10-one* (**6**). NaH (2.172 g, 90.24 mmol), obtained from the dispersion of NaH in oil, was added to dry DMSO (320 ml). Under intense stirring, trimethylsulfoxonium iodide (*Fluka*; 36.13 g, 164.2 mmol) was added within 5 min. The evolution of H_2 was indicated by transitory foaming. After additional stirring for 30 min, a soln. of **5** (12.00 g, 82.08 mmol) in dry DMSO (70 ml) was added dropwise within 40 min. The resulting dark brown mixture was heated for 1 h at 75°, whereby the color changed to light yellow. The cooled mixture was poured onto ice and extracted with CH_2Cl_2. After filtration over cotton wool, the solvent was distilled off, and the residue was subjected to CC (silica gel; hexane/Et_2O 2:1) to give pure **6** (9.60 g, 73%). Slightly yellow oil. R_f (hexane/Et_2O 2:1) 0.26. UV/VIS (hexane): λ_{max} 230 (3.56), 266 (3.60); λ_{min} 211 (3.41), 248 (3.52). IR (film): 3023*m*, 2935*m*, 2869*m*, 2835*w*, 1721v*s*, 1607*m*, 1435*m*, 1392*w*, 1348*w*, 1297*s*, 1262*m*, 1176*w*, 1088*m*, 1055*s*, 1019*m*, 924*w*, 851*m*, 820*w*, 779*m*, 707v*s*, 654*w*, 603*m*, 547*w*. ^{1}H-NMR: 6.47 (*d*, $^3J(2,3)=11.8$, H–C(2)); 5.86 (*ddd*, $^3J(4,5)=11.1$, $^3J(4,3)=6.0$, $^4J=2.0$, H–C(4)); 5.63 (*dd*, $^3J(3,2)=11.8$, $^3J(3,4)=6.0$, H–C(3)); 5.61–5.53 (*m*, H–C(5)); 2.69 (complex *ABX* system, $\delta_A-\delta_B\approx 8$, CH_2(6)); 2.58 (*d*, $^2J(11_b,11_a)=4.4$, H_b–C(11)); 2.19–2.01 (*m*, CH_2(8,9)); 1.25 (*dd*, $^2J(11_a,11_b)=4.4$, $^4J=0.9$, H_a–C(11)). ^{13}C-NMR: 211.92 (*s*, C(10)); 128.68, 127.43, 127.18, 122.78 (4*d*, C(2,3,4,5)); 58.06 (*s*, C(1)); 41.30 (*s*, C(7)); 32.47, 31.93, 28.14 (3*t*, C(6,8,9)); 22.60 (*t*, C(11)). GC/MS ($C_{11}H_{12}O$; 160.22): 160 (45, $M^{+\cdot}$), 145 (8), 133 (35), 117 (100), 104 (80), 91 (63), 78 (61), 77 (60).

1.1.4. *Tricyclo[5.3.1.0^{1,7}]undeca-2,4,9-triene* (**8**). 1.1.4.1. *Tricyclo[5.3.1.0^{1,7}]undeca-2,4-dien-10-one Tosylhydrazone* (**7**). Ketone **6** (8.63 g, 53.86 mmol) was dissolved in THF (13 ml) and $TsNHNH_2$ (10.64 g, 57.13 mmol) was added in portions at r.t. Stirring was continued for 15 h at r.t., and the pale yellow suspension obtained was filtered and washed with a small amount of ice-cold Et_2O. The now colorless powder of **7** was dried in h.v. (15.37 g, 87%). M.p. 190–192° ([2]: 190–192°). R_f(hexane/Et_2O 2:1) 0.13. UV (MeCN): λ_{max} 226 (3.95); λ_{min} 212 (3.87). IR (KBr): 3216v*s*, 3025*m*, 2933*m*, 1654*m*, 1599*w*, 1494*w*, 1436*m*, 1400*s*, 1343v*s*, 1310*m*, 1168v*s*, 1076*s*, 1023*s*, 927*m*, 850*w*, 816*s*, 710v*s*, 697*s*, 662*s*, 622*m*, 567v*s*, 549*s*. ^{1}H-NMR: 7.88 (*d*, $^3J=8.4$, H_o of Ph); 7.32 (*d*-like, $^3J=8.4$, H_m of Ph); 6.48 (*d*, $^3J(2,3)=12.0$, H–C(2)); 5.82 (*ddd*, $^3J(4,5)=11.3$, $^3J(4,3)=6.0$, $^4J=2.2$, H–C(4)); 5.56 (*dd*, $^3J(3,2)=12.0$, $^3J(3,4)=6.0$, H–C(3)); 5.52–5.47 (*m*, H–C(5)); 2.59 (complex *ABX* system, $\delta_A-\delta_B\approx 8$ Hz); 2.43 (*s*, Me–Ph)); 2.36 (*d*, $^2J(11_a,11_b)=4.6$, H_a–C(11)); 2.07–1.75 (*m*, CH_2(8,9)); 0.80 (*dd*, $^2J(11_b,11_a)=4.6$, $^4J=0.7$, H_b–C(11)). ^{13}C-NMR: 167.75 (*s*, C(10)); 143.82 (*s*, C_p of Ph)); 135.29 (*s*, C_{ipso} of Ph)); 129.75, 128.67, 127.61, 121.65 (4*d*, C(2,3,4,5)); 129.38 (*d*, C_m of Ph)); 128.08 (*d*, C_o of Ph)); 56.01 (*s*, C(1)); 37.01 (*s*, C(7)); 31.99, 30.87, 23.09 (3*t*, C(6,8,9)); 21.49 (*q*, Me–Ph); 20.96 (*t*, C(11)). EI-MS ($C_{18}H_{20}N_2O_2S$; 328.44): 328 (14, $M^{+\cdot}$), 173 (100, $[M-Ts]^{+\cdot}$), 144 (27, $[M-TsN_2H]^{+\cdot}$), 129 (96), 115 (32), 91 (68), 77 (18).

1.1.4.2. *Formation of* **8**. A 1.45M soln. of MeLi in Et_2O (188 ml, 0.273 mol) was added at r.t. within 1 h to a suspension of **7** (43.38 g, 0.132 mol) in Et_2O (860 ml). The evolution of CH_4 was indicated by foaming of the stirred mixture. The initially colorless mixture became yellow after addition of the first mol-equiv. of MeLi, and turned orange after the second mol-equiv. of MeLi. The elimination of N_2 was completed by stirring overnight at

r.t., whereby the mixture turned brown. H_2O (10 ml) was added under ice cooling, whereby the temp. of the mixture rose for a short time to 55°. Et_2O (200 ml) was added, and the mixture was 3 times washed with ice-cold H_2O. The waste H_2O was re-extracted with Et_2O (100 ml), and the combined Et_2O extracts were dried ($MgSO_4$). The light orange-colored residual oil of the Et_2O extracts was subjected to CC (silica gel; pentane) to give **8** as a colorless volatile oil (17.30 g, 91%). R_f(pentane) 0.68. UV (hexane): λ_{max} 221 (sh, 3.61), 279 (3.44); λ_{min} 251 (3.30). IR (film): 3017v*s*, 2905v*s*, 2832v*s*, 1600*s*, 1436*m*, 1287*w*, 1253*m*, 1195*m*, 1143*w*, 1122*w*, 1075*m*, 1034*m*, 938*s*, 902*m*, 848*m*, 805*m*, 740v*s*, 706*s*, 685v*s*, 623v*s*, 556*m*, 512*s*. ^{1}H-NMR (600 MHz, $CDCl_3$): 6.19 (*d*, $^3J(2,3) = 11.6$, H–C(2)); 5.89 (*dtd*, $^3J(10,9) = 5.5$, $^4J(10,8) = 1.8$, $^4J(10, H_a–C(11)) = 0.5$, H–C(10)); 5.80 (*ddd*, $^3J(4,5) = 11.2$, $^3J(4,3) = 6.0$, $^4J = 2.6$, H–C(4)); 5.55 (*ddd*, $^3J(5,4) = 11.2$, $^3J(5,6_{exo}) = 8.4$, $^3J(5,6_{endo}) = 4.4$, H–C(5)); 5.51 (*dd*, $^3J(3,2) = 11.6$, $^3J(3,4) = 6.0$, H–C(3)); 5.30 (*dt*, $^3J(9,10) = 5.5$, $^3J(9,8) = 2.2$, H–C(9)); 2.68 (*A* of *ABX*, $^2J_{AB} = 14.8$, $^3J(6,5) = 8.3$, H_{exo}–C(6)); 2.64 (*A* of *ABXY*, $^2J_{AB} = 17.4$, $^3J(8,9) \approx {}^4J(8, H_a–C(11)) = 2.2$, H_{endo}–C(8)); 2.60 (B part of the ABX system, br., $^2J_{AB} = 14.8$, H_{endo}–C(6)); 2.39 (*B* of *ABXY*, $^2J_{AB} = 17.4$, $^3J(8,9) \approx {}^4J(8, H_a–C(11)) = 2.2$, H_{exo}–C(8)); 2.35 (*d*, $^2J(11_a,11_b) = 3.4$, H_a–C(11)); 0.34 (*d*, $^2J(11_b,11_a) = 3.3$, H_b–C(11)). ^{13}C-NMR (150 MHz, $CDCl_3$): 138.47 (*d*, C(10)); 134.75 (*d*, C(2)); 128.68 (*d*, C(4)); 128.49 (*d*, C(5)); 125.65 (*d*, C(9)); 121.80 (*d*, C(3)); 52.94 (*s*, C(7)); 43.50 (*t*, C(8)); 38.65 (*s*, C(1)); 32.48 (*t*, C(6)); 24.90 (*t*, C(11)). GC/MS ($C_{11}H_{12}$, 144.22): 144 (92, $M^{+\cdot}$), 141 (78), 128 (99, $C_{10}H_8^+$), 115 (100), 103 (71), 91 (80), 77 (79).

1.1.5. *Bicyclo[5.3.1]undeca-2,4,9-triene-1,7-diyl Diacetate* (**9**). *General.* As mentioned already in the *Theor. Part*, the formation of **9** had been, in our hands, the most delicate step in the synthesis of **2**. Neither by varying the reaction conditions (*cf. Table 1*) nor by changing the batch of $Pb(OAc)_4$ (*Fluka*) could we attain the yield that had been reported by *Scott* and *Kirms* [5]. We describe here our run that delivered the highest yield.

Formation of **9**. To a mixture of benzene (270 ml) and glacial AcOH (110 ml) were added, at 15°, **8** (5.98 g, 41.46 mmol) and $Pb(AcO)_4$. The mixture was stirred during 1 h at 15°, whereby the initially colorless suspension turned yellow. Stirring was continued at r.t. during 15 h, and then a further amount of $Pb(AcO)_4$ (18 g, 40 mmol) was added. The run was terminated after 3 h stirring at 35°. Most of the solvent mixture was distilled off, and the remaining yellow suspension was filtered. The residue of the filtrate was passed through a short column (silica gel; hexane/*t*-BuOMe 4:1) and washed several times with H_2O to remove the last amounts of $Pb(AcO)_2$ and then with $NaHCO_3$ and sat. NaCl soln. After drying ($MgSO_4$), the residue of the org. phase was dissolved in toluene (50 ml), which was removed again by distillation. Finally, CC of the residue (silica gel; hexane/*t*-BuOMe 8:1) led to a colorless oil, which crystallized after a short time of standing at r.t. Recrystallization (hexane/TBME 10:1) gave pure **9** (3.05 g, 28%) as colorless crystals. M.p. 92–94°. R_f (hexane/TBME 6:1) 0.34. UV (hexane): λ_{max} 247 (3.63); λ_{min} 223 (3.33). IR (KBr): 2937*w*, 1726v*s*, 1434*m*, 1372v*s*, 1348*m*, 1330*w*, 1259v*s*, 1229v*s*, 1195*s*, 1144*w*, 1070*s*, 1049*s*, 1023*s*, 983*m*, 959v*s*, 943*s*, 915*m*, 880*s*, 828*m*, 793*s*, 763*m*, 744*s*, 724*w*, 689*w*, 662*w*, 632*m*, 605*w*, 575*w*. ^{1}H-NMR (600 MHz, $CDCl_3$): 6.15 (*dd*, $^3J(4,5) = 10.8$, $^3J(4,3) = 4.8$, H–C(4)); 5.79–5.77 (*m*, H–C(9)); 5.77 (*dd*, $^3J(3,2) = 12.8$, $^3J(3,4) = 4.9$, H–C(3)); 5.70–5.66 (*m*, H–C(5), H–C(10)); 5.46 (*dd*, $^3J(2,3) = 12.5$, $^4J = 1.8$, H–C(2)); 3.51 (*d*, $^2J(11_a,11_b) = 12.8$, H_a–C(11)); 2.86 (br. *t*-like, $J = 2.6$, CH_2(8)); 2.82 (*ddd*, *A* of *ABX*, $^2J_{AB} = 13.8$, $^3J_{AX} = 7.0$, $^4J = 1.5$, CH_2(6)); 2.77 (*dd*, *B* of *ABX*, $^2J_{AB} = 13.8$, $^3J_{BX} = 9.1$, CH_2(6)); 2.30 (*dt*, $^2J(11_b,11_a) = 12.8$, $^4J = 1.7$, H_b–C(11)); 1.984, 1.977 (2*s*, 2 MeOCO). ^{13}C-NMR (150 MHz, $CDCl_3$): 170.43, 169.67 (2*s*, 2 MeO*C*O); 130.60 (*d*, C(2)); 129.92, 129.90 (2*d*, C(4,10)); 128.46 (*d*, C(5)); 127.18 (*d*, C(9)); 125.24 (*d*, C(3)); 84.02, 83.86 (2*s*, C(1,7)); 36.75, 36.74 (2*t*, C(8,11)); 33.47 (*t*, C(6)); 22.44, 22.39 (2*q*, MeOCO–C(1,7)). GC/MS: 262 (15, $M^{+\cdot}$), 202 (5, $[M - AcOH]^{+\cdot}$), 160 (100, $[M + H - (AcOH + MeCO]^{+\cdot}$), 142 (55, $[M - 2\ AcOH]^{+\cdot}$), 131 (33), 117 (41), 115 (21), 104 (8), 91 (27), 77 (9). Anal. calc. for $C_{15}H_{18}O_4$ (262.31): C 68.68, H 6.92; found: C 68.77, H 6.95.

In addition, the structure of **9** was established by an X-ray crystal-structure analysis (*cf. Fig. 2* and *Table 9*).

1.1.6. *Formation of* **2**. Since the last intermediates on the way to **2** were quite unstable, the following steps were performed one after the other.

1.1.6.1. *Bicyclo[5.3.1]undeca-2,4,8,10-tetraen-7-yl Acetate* (**10**). To a soln. of **9** (5.03 g, 19.18 mmol) in heptane (250 ml) were added under stirring at r.t. in the following order: $Pd(OAc)_2$ (0.077 g, 0.34 mmol), Ph_3P (0.56 g, 2.14 mmol), and Na_2CO_3 (1.87 g, 12.4 mmol). The slightly yellow mixture was stirred at 85° during 15 h, which led to a light yellow suspension. After filtration over *Celite*, most of the solvent was distilled off. The residue was subjected to CC (silica gel; hexane/*t*-BuOMe 50:1) to give pure **10** (3.71 g, 96%). Unstable, bright yellow oil. R_f (hexane/*t*-BuOMe 20:1) 0.47. IR (film): 3014*s*, 2935*m*, 1737v*s*, 1550*w*, 1449*s*, 1369v*s*, 1282*s*, 1234v*s*, 1131*w*, 1052v*s*, 1020*s*, 985*m*, 859*m*, 830*w*, 746*s*, 709*s*, 641*m*, 606*m*, 579*w*, 557*w*, 497*w*. ^{1}H-NMR: 6.10–6.06 (*m*, H–C(2,8)); 5.90 (*ddd*, $^3J(4,5) = 12.1$, $^3J(4,3) = 6.4$, $^4J = 1.8$, H–C(4)); 5.83 (*dd*, $^3J(9,8) = 9.3$, $^3J(9,10) = 4.4$, H–C(9)); 5.59 (*d*, $^3J(10,9) = 4.4$, H–C(10)); 5.51–5.44 (*m*, H–C(3,5)); 4.04 (*ddd*, *A* of *ABX*, $^2J_{AB} = 14.1$,

$^3J_{AX}$ = 8.5, ^4J = 1.3, H_{endo}–C(6))[9]; 3.57 (*s*, CH_2(11)); 2.38 (*dd*, *B* of *ABX*, $^2J_{AB}$ = 14.1, $^3J_{BX}$ = 7.9, H_{endo}–C(6)); 2.04 (*s*, MeOCO). ^{13}C-NMR: 170.51 (*s*, MeO*C*O); 138.95 (*s*, C(1)); 136.10, 131.13, 128.97, 127.78, 126.04, 125.00, 122.92 (7*d*, C(2)–C(5), C(8)–C(10)); 84.71 (*s*, C(7)); 34.42, 31.73 (2*t*, C(6,11)); 21.95 (*q*, *Me*OCO). GC/MS ($C_{13}H_{14}O_2$; 202.26): 202 (33, $M^{+\cdot}$), 160 (82), 159 (78, $[M - MeCO]^+$), 145 (100), 142 (79, $[M - AcOH]^{+\cdot}$), 141 (92), 127 (93), 115 (96), 103 (21), 91 (3), 77 (73).

1.1.6.2. *Bicyclo[5.3.1]undeca-2,4,8,10-tetraene-7-ol* (**11**). To a soln. of freshly prepared **10** (3.71 g, 18.34 mmol) in Et_2O (80 ml) was dropped at r.t. and within 30 min a 1.45M soln. of MeLi in Et_2O (26.2 ml, 38 mmol). Stirring was continued for 1 h. The now brown suspension was cooled with ice, and H_2O (*ca.* 50 ml) was added. The aq. phase was extracted with Et_2O (3×), and the combined org. layers were washed with sat. NaCl soln. After drying (Na_2SO_4) and removal of the solvent, the residue was further dried and freed from traces of solvent in h.v. Alcohol **11** was obtained as a pale yellow, unstable oil (2.64 g, 90%). A sample of **11** was further purified by chromatography (alumina; hexane/*t*-BuOMe 2:1). R_f (hexane/*t*-BuOMe 2:1) 0.21. IR (film): 3359v*s*, 3013v*s*, 2973v*s*, 1713v*w*, 1589*m*, 1548*w*, 1477*s*, 1374v*s*, 1278*s*, 1231*s*, 1204*s*, 1083v*s*, 1015*s*, 988*m*, 926*s*, 871*m*, 857*s*, 830*w*, 740v*s*, 708v*s*, 653*m*, 613*m*, 559*s*, 478v*w*. ^{1}H-NMR: 6.08 (*d*, ^3J(2,3) = 11.8, H–C(2)); 5.89 (*ddd*, ^3J(4,5) = 12.2, ^3J(4,3) = 6.3, ^4J = 1.7, H–C(4)); 5.83 (*dd*, ^3J(9,8) = 9.4, ^3J(9,10) = 4.9, H–C(9)); 5.73 (*d*-like, ^3J = 8.4, H–C(8)); 5.59–5.52 (*m*, H–C(5, 10)); 5.46 (*dd*, ^3J(3,2) = 11.8, ^3J(3,4) = 6.3, H–C(3)); 4.04 (*dd*, *A* of *ABX*, $^2J_{AB}$ = 13.6, $^3J_{AX}$ = 8.4, H_{endo}–C(6)); 3.62, 3.07 (2*d*, *AB*, $^2J_{AB}$ = 11.9, CH_2(11)); 1.88 (*ddd*, *B* of *ABX*, $^2J_{AB}$ = 13.6, $^3J_{BX}$ = 8.0, ^4J = 1.7, H_{exo}–C(6)); 1.67 (*s*, OH). ^{13}C-NMR: 140.24, 131.13, 128.99, 128.17, 125.65, 125.44, 123.04 (7*d*, C(2–5), C(8–10)); 139.49 (*s*, C(1)); 76.56 (*s*, C(7)); 37.88, 35.08 (2*t*, C(6,11)). GC/MS ($C_{11}H_{12}O$; 160.22): 160 (77, $M^{+\cdot}$), 159 (74, $[M - H]^+$), 145 (92), 142 (30, $[M - H_2O]^+$), 131 (81), 127 (89), 115 (100), 103 (71), 91 (80), 77 (81).

1.1.6.3. *Bicyclo[5.3.1]undeca-2,4,8,10-tetraen-7-yl Methanesulfonate* (**12**). Freshly prepared **11** (2.63 g, 16.41 mmol), dissolved in CH_2Cl_2 (90 ml) was cooled to 0°. At this temp., Et_3N (9.2 ml, 66.0 mmol) and then MsCl (2.55 ml, 32.81 mmol) were added. The dark yellow mixture was stirred during 1 h at r.t. To hydrolyze the excess MsCl, ice-cold 0.25M HCl (100 ml) was added. The org. phase was washed (2×) with sat. aq. $NaHCO_3$ and with H_2O. The soln. was filtered over cotton wool, and the solvent was distilled off. The dark brown residue was dissolved in a 1:1 mixture of hexane/*t*-BuOMe and filtered over alumina to give **12** (3.79 g, 97%). Yellow, very unstable oil. R_f(hexane/TBME 2:1) 0.34. IR (film): 3016*m*, 2936*m*, 1607*w*, 1447*m*, 1338v*s*, 1279*w*, 1175v*s*, 1129*m*, 1039*m*, 1010*m*, 966*s*, 920v*s*, 853*s*, 784*s*, 747*s*, 719*s*, 651*w*, 568*m*, 521*m*, 448*w*. ^{1}H-NMR: 6.28 (*dd*, ^3J(8,9) = 9.3, ^4J = 1.9, H–C(8)); 6.10 (*d*, ^3J(2,3) = 11.9, H–C(2)); 5.63 (*ddd*, ^3J(4,5) = 12.2, ^3J(4,3) = 6.5, ^4J = 1.8, H–C(4)); 5.89 (*dd*, ^3J(9,8) = 9.3, ^3J(9,10) = 4.4, H–C(9)); 5.63–5.58 (*m*, H–C(5,10)); 4.14 (*dd*, *ABX*, $^2J_{AB}$ = 14.6, $^3J_{AX}$ = 8.5, H_{endo}–C(6)); 3.81 (*dd*, *A* of *AB*, $^2J_{AB}$ = 11.9, ^4J = 1.9, CH_2(11)); 3.59 (*d*, *B* of *AB*, $^2J_{AB}$ = 11.9, CH_2(11)); 3.06 (*s*, $MeOSO_2$); 2.44 (*ddd*, *B* of *ABX*, $^2J_{AB}$ = 14.6, $^3J_{BX}$ = 7.8, ^4J = 2.0, H_{exo}–C(6)). ^{13}C-NMR: *ca.* 138 (*s*, C(1)); 135.10, 128.57, 126.84, 126.11, 123.32 (7*d*, C(2)–C(5), C(8)–C(10)); *ca.* 77 (*s*, C(7)); 40.41 (*q*, *Me*OSO_2); 35.78, 33.00 (2*t*, C(6,11)). GC/MS ($C_{12}H_{14}O_3S$; 238.31): 238 (83, $M^{+\cdot}$), 159 (89, $[M - MeSO_2]^+$), 142 (34, $[M - MsOH]^{+\cdot}$), 141 (67), 131 (100), 115 (88), 103 (21), 91 (86), 77 (33).

1.1.6.4. *Elimination of MsOH from* **12**. To a soln. of freshly prepared **11** (3.37 g, 14.14 mmol) in Et_2O (100 ml) was added 1,5-diazabicyclo[4.3.0]non-5-ene (DBN; 8.5 ml, 71.2 mmol) at r.t. After stirring during 1 h, the initially yellow soln. turned orange, and the formation of a brown, polymer-like precipitate was observed. Stirring was continued during 15 h at r.t. After addition of a second amount of DBN (4.0 ml, 33.5 mmol), stirring was continued for 2 additional h. Then, the now dark orange-colored mixture was diluted with pentane (200 ml), poured on ice, and washed several times with sat. aq. NaCl soln. After drying (Na_2SO_4) and careful removal of the solvent mixture by distillation, the brown-to-orange-colored residue was subjected to CC (alumina; pentane) to yield **2** (1.07 g, 53%). Orange-colored, volatile and unstable oil. R_f (pentane) 0.70. UV/VIS (hexane): λ_{max} 257 (sh, 4.12), 281 (4.54), 297 (sh, 3.96), 326 (3.65), 485 (2.63); λ_{min} 228 (3.79), 315 (3.63). IR (film): 3015*s*, 2920*m*, 2864*m*, 1508*w*, 1456*s*, 1399*w*, 1369*w*, 1306*w*, 1248*m*, 1223*w*, 1078v*w*, 1031*w*, 984*m*, 897*s*, 858*m*, 839*m*, 759v*s*, 685*s*, 656v*s*, 570*m*. ^{1}H-NMR (600 MHz, (D_6)acetone; see *Fig. 2*): 8.13 (*d*, ^3J(2,3) = ^3J(6,5) = 9.0, H–C(2,6)); 7.55 (*d*, ^3J(8,9) = ^3J(8,10) = 7.1, H–C(8,10)); 7.38 (*td*, ^3J(4,3) = ^3J(4,5) = 11.1, ^4J = 0.9, H–C(4)); 7.31 (*dd*, ^3J(3,4) = ^3J(5,4) = 11.0, ^3J(3,2) = ^3J(5,6) = 8.3, H–C(3,5)); 6.88 (*t*, ^3J(9,8) = ^3J(9,10) = 7.2, H–C(9)); –0.75 (*d*, ^2J(11_b,11_a) = 9.8, H_b–C(11)); –1.22 (*dt*, ^2J(11_a, 11_b) = 9.8, ^4J(11_a,8) = ^4J(11_a, 10) = 1.6, H_a–C(11).

---

[9]) AM1 Calculations of the lowest-energy conformation of **10** show H_{endo}–C(6) in a more or less co-linear arrangement with H–C(5) (Θ(H–C(5)–C(6)–H_{endo}) = 18°), *i.e.*, it lies almost in the π-plane of the adjacent C=C bond, whereas H_{exo}–C(6) extends into the π-cloud of the tetraene system (Θ(H–C(5)–C(6)–H_{exo}) = –136°). These structural features explain well the large chemical-shift difference between H_{endo} and H_{exo}.

^{13}C-NMR (150 MHz, (D_6)acetone): 160.64 (*s*, C(1,7)); 143.53 (*d*, C(2,6)); 132.97 (*d*, C(8,10)); 129.77 (*d*, C(9)); 128.35 (*d*, C(4)); 124.89 (*d*, C(3,5)); 34.63 (*t*, C(11)). GC/MS ($C_{11}H_{10}$; 142.20): 142 (75, $M^{+\cdot}$), 141 (99), 139 (66), 126 (10), 115 (100, [C_9H_7 (= inden-1-yl)]$^+$), 102 (19), 98 (7), 91 (15), 89 (65), 87 (26), 77 (22), 74 (32), 70 (26), 65 (32), 63 (68), 57 (30), 51 (57).

1.2. *Bicyclo[5.3.1]undeca-1,3,5,7,9-pentaene-8-carbaldehyde* (= *Homoazulene-8-carbaldehyde*; **27**). The *Vilsmeyer* reagent was prepared from DMF (4 ml) and $POCl_3$ (0.825 ml, 9.00 mmol) at 0°. It was added dropwise with a syringe to a vigorously stirred soln. of **2** (1.067 g, 7.50 mmol) in DMF (6 ml). A change of the color of the mixture from orange to dark red was observed. After 15 min, ice-cold H_2O (20 ml) was added, and the mixture was neutralized with 4N aq. NaOH. The aq. phase was extracted (3×) with CH_2Cl_2, and the combined org. layers were washed (2×) with 4N NaOH and once with sat. aq. $NaHCO_3$ soln. After filtration over cotton wool, the solvent was distilled off, and the residue, which still contained DMF, was freed from the latter in h.v. at 45°. CC (silica gel; hexane/*t*-BuOMe 3:1) provided pure **27** (0.856 g, 67%). Red, unstable oil. R_f (hexane/TBME 3:1) 0.34. UV/VIS (MeCN): λ_{max} 218 (4.10), 238 (4.12), 293 (4.25), 378 (3.82); λ_{min} 202 (3.98), 225 (4.08), 257 (3.96), 341 (3.59). IR (film): 3020*w*, 2818*w*, 2719*w*, 1659v*s*, 1566*w*, 1473*s*, 1427*m*, 1347*w*, 1227*s*, 1207*s*, 1075*w*, 980*m*, 905*w*, 873*w*, 804*s*, 762*m*, 721*w*, 659*s*, 616*m*, 589*w*, 551*w*, 525v*w*. ^{1}H-NMR (600 MHz, $CDCl_3$): 10.05 (*s*, CHO)); 8.66 (*d*, ^3J(6,5) = 8.9, H–C(6)); 8.12 (*d*, ^3J(2,3) = 8.6, H–C(2)); 7.55 (*d*, ^3J(9,10) = 7.2, H–C(9)); 7.53 (*dd*, ^3J(10.4, ^3J = 8.9, H–C(5)); 7.49–7.44 (*m*, H–C(3,4,10)); −0.03 (*d*, ^2J(11_b, 11_a) = 9.9, H_b–C(11)); −1.00 (*dd*, ^2J(11_a, 11_b) = 9.9, ^4J(11_a, 10) = 1.6, H_a–C(11). ^{13}C-NMR (150 MHz, $CDCl_3$): 187.10 (*d*, CHO)); 158.65 (*s*, C(1)); 154.51 (*s*, C(7)); 143.72 (*d*, C(6)); 143.20 (*d*, C(2)); 141.18 (*s*, C(8)); 136.30 (*d*, C(9)); 130.16 (*d*, C(10)); 128.68 (*d*, C(4)); 128.10 (*d*, C(5)); 126.60 (*d*, C(3)); 34.84 (*t*, C(11)). GC/MS ($C_{12}H_{10}O$; 170.21): 170 (32, $M^{+\cdot}$), 169 (27, [$M-1$]$^+$), 141 (100, [M – CHO]$^+$), 139 (34), 126 (3), 115 (66), 102 (4), 91 (4), 89 (22), 77 (6), 63 (18).

The formation of azulene under the same conditions as described above gave azulene-1-carbaldehyde as a violet oil in a yield of 96%.

1.3. *8-[(*E*)- and (*Z*)-2-Phenylethenyl]bicyclo[5.3.1]undeca-1,3,5,7,9-pentaene* (= *8-[(*Z*)-* and (E)*-2-Phenylethenylhomoazulene; (*Z*)*-**28** and (*E*)-**28**). To a suspension of benzyl(triphenyl)phosphonium chloride (2.29 g, 5.89 mmol) in THF (11 ml) was added at r.t. *t*-BuOK (0.70 g, 6.24 mmol) in THF (22 ml). The red ylide soln. prepared was stirred during 1 h at r.t. and then cooled to −78°. A soln. of **27** (0.310 g, 1.82 mmol) in THF (10 ml) was added, and stirring was continued during 15 min at −78°. The *Wittig* reaction was completed by stirring at r.t. during 1 h. H_2O (10 ml) and Et_2O (*ca.* 50 ml) were added, and the org. layer was washed with sat. aq. $NaHCO_3$ soln. and then dried (Na_2SO_4). The solvent mixture was concentrated until Ph_3PO had precipitated. It was filtered and washed with Et_2O. The filtrate was concentrated again, the residue taken up in hexane and filtered over a short alumina column to give a 1.6:1 mixture of (*Z*)-**28** and (*E*)-**28** (0.440 g, 99%) as a red unstable oil. For the separation of the (*Z*)- and (*E*)-isomers, the mixture was carefully chromatographed on alumina (400 g) with hexane to give, as a first fraction, pure (*Z*)-**28** (0.093 g), followed by a larger mixed fraction of (*Z*)-**28** and (*E*)-**28**. Finally, pure (*E*)-**28** (0.075 g) was obtained as a third fraction.

*Data of (*Z*)-***28***: Dark red oil. R_f (hexane) 0.31. UV/VIS (hexane): λ_{max} 224 (4.27), 264 (4.38), 304 (4.35), 384 (3.95), 484 (sh, 2.79); λ_{min} 215 (4.24), 243 (4.20), 277 (4.14), 343 (3.63). IR (film): 3019*s*, 2862*w*, 1598*m*, 1572v*w*, 1492*s*, 1446*s*, 1250*w*, 1179v*w*, 1155v*w*, 1074*w*, 1028*w*, 961*w*, 918*m*, 872*w*, 820*m*, 774v*s*, 695v*s*, 663v*s*, 630*w*, 614*w*, 544*m*, 479*w*. ^{1}H-NMR (600 MHz, (D_6)acetone): 8.13 (*d*, ^3J(2,3) = 8.2, H–C(2)); 7.73 (*d*, ^3J(6,5) = 8.4, H–C(6)); 7.50 (*d*, ^3J(7.5, H_o of Ph); 7.28–7.26 (*m*, H_m of Ph, H–C(10)); 7.20–7.15 (*m*, H_p of Ph, H–C(3,4)); 7.02–6.99 (*m*, H–C(5)); 6.77 (*d*, *A* of *AB*, $^2J_{AB}$ = 12.0, H–C(1′)); 6.74 (*d*, ^3J(9,10) = 7.1, H–C(9)); 6.51 (*d*, *B* of *AB*, $^2J_{AB}$ = 12.0, H–C(2′)); −0.19 (*d*, ^2J(11_b, 11_a) = 9.8, H_b–C(11)); −0.89 (*dd*, ^2J(11_a, 11_b) = 9.8, ^4J(11_a, 10) = 1.4, H_a–C(11). ^{13}C-NMR (150 MHz, (D_6)acetone): 157.58 (*s*, C(1)); 156.48 (*s*, C(7)); 144.02 (*d*, C(2)); 143.24 (*s*, C(8)); 140.64 (*d*, C(6)); 139.22 (*s*, C_{ipso} of Ph); 131.46 (*d*, C(10)); 130.59 (*d*, C(9)); 129.74 (*d*, C_o of Ph); 129.30 (*d*, C(2′)); 129.10 (*d*, C_m of Ph); 128.26 (*d*, C(4)); 127.92 (*d*, C_p of Ph); 126.99 (*d*, C(1′)); 125.27 (*d*, C(3)); 125.16 (*d*, C(5)); 34.67 (*t*, C(11)). GC/MS ($C_{19}H_{16}$; 244.34): 244 (90, $M^{+\cdot}$), 243 (89, [M – H]$^+$), 228 (90), 215 (88), 202 (87), 189 (61), 165 (98), 152 (79), 141 (87), 139 (76), 128 (65), 121 (52), 115 (100), 114 (82), 107 (48), 102 (52), 91 (81), 77 (72).

*Data of (*E*)-***28***: Red oil. R_f (hexane) 0.18. UV/VIS (hexane): λ_{max} 228 (4.25), 263 (4.25), 314 (4.36), 399 (4.24); λ_{min} 214 (4.13), 245 (4.12), 276 (4.06), 343 (3.72). IR (film): 3023*s*, 2955*m*, 2923*m*, 2866*m*, 1796v*w*, 1594*s*, 1495*s*, 1447*s*, 1251*m*, 1155v*w*, 1072*w*, 1028*w*, 958v*s*, 897*m*, 814*s*, 796*m*, 777v*s*, 717v*s*, 692v*s*, 658v*s*, 616*s*, 548*s*, 496*w*. ^{1}H-NMR (500 MHz, (D_6)acetone): 8.21 (*d*, ^3J(2,3) = 9.6, H–C(2)); 7.98 (*d*, ^3J(6,5) = 7.1, H–C(6)); 7.67 (*d*, ^3J(7.5, H_o of Ph); 7.63 (*d*, ^3J(1′,2′) = 16.4, H–C(1′)); 7.40 (*t*, ^3J = 7.7, H_m of Ph); 7.31 (*d*, ^3J(2′,1′) = 16.4, H–C(2′)); 7.31–7.25 (*m*, H_p of Ph, H–C(10)); 7.21–7.17 (*m*, H–C(4), H–C(5)); 7.11 (*t*, ^3J = 9.7, H–C(3)); 6.92 (*d*, ^3J(9,10) = 6.6, H–C(9)); −0.03 (*d*, ^2J(11_b, 11_a) = 9.8, H_b–C(11)); −0.25 (*dd*, ^2J(11_a, 11_b) = 9.8, ^4J(11_a,

10) = 1.2, H_a–C(11)). ^{13}C-NMR (125 MHz, (D_6)acetone): 156.62 (*s*, C(1)); 154.93 (*s*, C(7)); 146.08 (*s*, C(8)); 145.01 (*d*, C(2)); 140.11 (*d*, C(6)); 138.63 (*s*, C_{ipso} of Ph); 130.54 (*d*, C(10)); 129.51 (*d*, C_m of Ph); 128.90 (*d*, C(2′)); 128.79 (*d*, C(4)); 128.13 (*d*, C_p of Ph); 127.18 (*d*, C_o of Ph); 126.41, 126.37 (2*d*, C(1′) and C(9)); 125.48 (*d*, C(5)); 124.86 (*d*, C(3)); 35.15 (*t*, C(11)). GC/MS ($C_{19}H_{16}$; 244.34): 244 (67, $M^{+\cdot}$), 243 (60, $[M-H]^+$), 228 (78), 226 (77), 215 (88), 202 (81), 189 (53), 178 (7), 165 (85), 152 (70), 141 (87), 139 (77), 128 (55), 121 (36), 115 (100), 114 (77), 102 (47), 91 (80), 77 (66).

2. Homoheptalene-dicarboxylates. – 2.1. *Dimethyl Bicyclo[5.5.1]trideca-1,3,5,7,9,11-hexaene-2,3-* and *-4,5-dicarboxylate* (= *Dimethyl Homoheptalene-2,3-* and *-4,5-dicarboxylate*; **13** and **3**, resp.). Homoazulene (**2**; 0.117 g, 0.823 mmol) was dissolved in $ClCH_2CH_2Cl$ (0.5 ml) under Ar in a *Schlenk* vessel. ADM (0.30 ml, 2.44 mmol) was added to the orange-colored soln., which was heated under Ar during 30 h at 82°. $ClCH_2CH_2Cl$ and the excess of ADM was removed from the now brown-red mixture at 50° in h.v. The residue was subjected to CC (silica gel; hexane/*t*-BuOMe 2:1) to give a 4:1 mixture of **3** and **13** (0.225 g, 96%) as a blood-red oil. For the separation of **3** and **13**, the mixture was again carefully chromatographed on silica gel (400 g) with hexane/*t*-BuOMe 4:1. This led to a fraction of strongly enriched **3**, from which pure **3** crystallized (0.090 g) after it had been dissolved in hexane/*t*-BuOMe 10:1. The combined residues (from CC and the mother liquor of crystallization) were once more chromatographed on silica gel (400 g) with hexane/*t*-BuOMe 4:1. Finally, from fractions enriched in **13**, the latter homoheptalene was obtained in pure crystalline form (9 mg) by crystallization from hexane/*t*-BuOMe 15:1.

Data of **3**: Red-orange prisms. M.p. 139–140° (hexane/*t*-BuOMe) ([2]: 139°). R_f(hexane/TBME 2:1) 0.180. UV/VIS (hexane): λ_{max} 270 (4.56), 330 (sh, 3.65), 419 (v. br.; 2.67); λ_{min} 212 (4.03), 392 (2.63). IR (KBr): 3006*w*, 2950*w*, 1725v*s*, 1700v*s*, 1610*s*, 1435*s*, 1377*w*, 1301*m*, 1275v*s*, 1243v*s*, 1069v*s*, 1045*s*, 994*m*, 954*w*, 934*m*, 885*m*, 865*m*, 854*m*, 789*s*, 764*w*, 753*m*, 723*s*, 699*w*, 669*w*, 653*w*, 560*w*, 522*w*, 482v*w*. ^{1}H-NMR (600 MHz, $CDCl_3$; see *Fig. 4,a*, and *Table 2*): 7.19 (*s*, H–C(6)); 6.99 (*d*, $^3J(3,2) = 4.$, H–C(3)); 6.11 (*d*, $^3J(8,9) = 4.7$, H–C(8)); 6.09 (*d*, $^3J(12,11) = 12.3$, H–C(12)); 5.92 (*d*, $^3J(2,3) = 4.3$, H–C(2)); 5.67 (*dd*, $^3J(9,10) = 11.5$, $^3J(9,8) = 4.8$, H–C(9)); 5.61 (*dd*, $^3J = 6.6$, H–C(11)); 5.60 (*dd*, $^3J(10,9) = 11.5$, $^3J(10,11) = 5.5$, H–C(10)); 5.07 (*d*, $^2J_{AB}$ = 11.3, *A* of *AB*, H_{syn}–C(13)); 4.97 (*d*, $^2J_{AB} = 11.3$, *B* of *AB*, H_{anti}–C(13)); 3.71 (*s*, MeOCO–C(4)); 3.68 (*s*, MeOCO–C(5)). ^{13}C-NMR (150 MHz, $CDCl_3$): 168.45 (*s*, MeO*C*O–C(5)); 167.55 (*s*, MeO*C*O–C(4)); 145.19 (*s*, C(1)); 144.35 (*d*, C(6)); 144.11 (*d*, C(3)); 143.87 (*s*, C(7)); 137.16 (*d*, C(8)); 135.97 (*d*, C(12)); 130.43 (*d*, C(9)); 130.36 (*s*, C(5)); 130.26 (*s*, C(4)); 129.49 (*d*, C(10)); 129.28 (*d*, C(11)); 125.99 (*d*, C(2)); 52.22 (*q*, *Me*OCO–C(5)); 52.09 (*q*, *Me*OCO–C(4)); 31.65 (*t*, C(13)). GC/MS ($C_{17}H_{16}O_4$; 284.32): 284 (96, $M^{+\cdot}$), 259 (5), 253 (60, $[M-MeO]^+$), 252 (32, $[M-MeOH]^{+\cdot}$), 237 (22), 225 (87, $[M-COOMe]^+$), 224 (82), 209 (67), 193 (79), 181 (50), 166 (70, $[M-2\,COOMe]^{+\cdot}$), 165 (100), 164 (82), 163 (78), 153 (80), 152 (85), 139 (82), 127 (75), 115 (81), 102 (18), 91 (22), 89 (28),77 (32).

In addition, the structure of **3** was determined by an X-ray crystal-structure analysis (*cf. Fig. 5,a* and *Tables 3* and *8*).

Data of **13**: Red prisms. M.p. 108–112°. R_f (hexane/*t*-BuOMe 2:1) 0.182. UV/VIS (hexane): λ_{max} 279 (4.51), 420 (v. br.; 2.70); λ_{min} 222 (3.98), 382 (2.64). IR (KBr): 3417v*w*, 3007*w*, 2957*m*, 2925*w*, 2853*w*, 1719v*s*, 1703v*s*, 1627*m*, 1610*w*, 1597*m*, 1584*w*, 1564*s*, 1535*w*, 1447*m*, 1428*s*, 1369*w*, 1263v*s*, 1244v*s*, 1203v*s*, 1154*s*, 1118*s*, 1059*s*, 1039*s*, 1005*m*, 982*m*, 941*m*, 921*w*, 903*m*, 893*w*, 879*m*, 860*m*, 840*w*, 822*m*, 797*m*, 785*s*, 738*m*, 727*m*, 712*w*, 676*m*, 651*m*, 622*w*, 574*w*, 537v*w*, 519v*w*, 503v*w*, 457v*w*. ^{1}H-NMR (600 MHz, $CDCl_3$; see *Fig. 4, b*, and *Table 3*): 7.71 (*d*, $^3J(12,11) = 12.9$, H–C(12)); 6.93 (*d*, $^3J(4,5) = 6.4$, H–C(4)); 6.00 (*ddd*, $^3J(11,12) = 12.9$, $^3J(11,10) = 7.6$, ^4J = 0.9, H–C(11)); 5.99 (*d*, $^3J(8,9) = 5.2$, H–C(8)); 5.99 (*d*, $^3J(6,5) = 12.8$, H–C(6)); 5.86 (*dd*, $^3J(9,10) = 12.2$, $^3J(9,8) = 5.2$, H–C(9)); 5.72 (*dd*, $^3J(10,9) = 12.2$, $^3J(10,11) = 5.2$, H–C(10)); 5.68 (*dd*, $^3J(5,6) = 12.8$, $^3J(5,4)$ = 6.4, H–C(5)); 5.41 (*dd*, *A* of *ABX*, $^2J_{AB} = 11.1$, $^4J_{AX} = 1.2$, H_{syn}–C(13)); 4.55 (*dd*, *B* of *ABX*, $^2J_{AB} = 11.1$, $^4J_{BX}$ = 0.8, H_{anti}–C(13)); 3.69 (*s*, MeOCO–C(3)); 3.68 (*s*, MeOCO–C(2)). ^{13}C-NMR (150 MHz, $CDCl_3$): 167.20 (*s*, MeO*C*O–C(3)); 166.98 (*s*, MeO*C*O–C(2)); 154.55 (*s*, C(1)); 143.80 (*s*, C(7)); 140.76 (*d*, C(4)); 137.06 (*d*, C(6)); 133.98 (*s*, C(3)); 133.70 (*d*, C(8)); 132.56 (*d*, C(11)); 131.88 (*d*, C(9)); 130.23 (*d*, C(12)); 128.48 (*d*, C(10)); 128.08 (*s*, C(2)); 127.54 (*d*, C(5)); 52.18 (*q*, *Me*OCO–C(2)); 51.51 (*q*, *Me*OCO–C(3)); 34.78 (*t*, C(13)). GC/MS ($C_{17}H_{16}O_4$; 284.32): 284 (35, $M^{+\cdot}$), 252 (9, $[M-MeOH]^{+\cdot}$), 237 (10), 225 (20, $[M-COOMe]^+$), 209 (10), 193 (13), 181 (9), 166 (58, $[M-2\,COOMe]^{+\cdot}$), 165 (100), 164 (35), 163 (28), 152 (32), 139 (20), 128 (10), 115 (19), 77 (5).

In addition, the structure of **13** was determined by an X-ray crystal-structure analysis (*cf. Fig. 5, b*, and *Tables 3* and *8*).

2.1.1. *Dimethyl (+)-(p*R*)- and (–)-(p*S*)-Homoheptalene-4,5-dicarboxylate* ((p*R*)-**3** and (p*S*)-**3**). Compound (±)-**3** of 2.1 (11.8 mg) was separated on a semi-prep. *Chiralcel OD* column (250 × 20 mm) with hexane/i-PrOH (20%) as eluant and a flow rate of 9 ml/min, which led to (+)-(p*R*)-**3** (4.7 mg) in the first fraction and

(−)-(p*S*)-**3** (5.2 mg) in the second one. Both enantiomers were obtained as a red oil. Attempts for crystallization were not undertaken.

*Data of (+)-(p*R*)-***3***:* t_R (conditions see above) 21.0 min. CD (hexane; r.t.; *cf. Fig. 6*): 425 (br., pos. max.; 6.04), 364 (pos. min.; 3.60), *ca*. 330 (pos. sh; 6.0), 296 (pos. max.; 7.97), 281 (0), 273 (neg. max.; 5.92), 264 (0), 258.5 (pos. max.; 4.03), 244 (pos. min.; 0.97), 227.5 (pos. max.; 10.98).

*Data of (−)-(p*S*)-***3***:* t_R (conditions see above) 56.0 min. CD (hexane; r.t.; *cf. Fig. 6*): 424 (br., neg. max.; 5.77), 364 (neg. min.; 3.58), *ca*. 325 (neg. sh; 6.7); 295.5 (neg. max.; 8.43), 281 (0), 272.5 (pos. max.; 5.18), 264 (0), 256 (neg. max.; 4.80), 244 (neg. min.; 1.89), 228 (neg. max.; 11.00).

2.2. *Dimethyl 2-[(*Z*)- and (*E*)-2-Phenylethenyl]bicyclo[5.5.1]trideca-1,3,5,7,9,11-hexaene-4,5-dicarboxylate (= Dimethyl 2-[(*Z*)- and (*E*)-2-Phenylethenyl]homoheptalene-4,5-dicarboxylate*; (*Z*)-**29** and (*E*)-**29**). The 1.6 : 1 mixture of (*Z*)-**28** and (*E*)-**28** (0.221 g, 0.904 mmol) was dissolved in $ClCH_2CH_2Cl$ (2.0 ml) in a *Schlenk* vessel. ADM (0.34 ml, 2.39 mmol) was added, and the stirred mixture was heated under Ar during 18 h at 82°, whereby the color of the mixture changed from red to brown. The solvent and the excess ADM were removed at 50° in h.v. The residue was subjected to CC (silica gel; hexane/TBME 3 : 1) to give a 5 : 1 mixture of (*Z*)-**29** and (*E*)-**29** as a brown-red oil (0.147 g, 42%). For the separation of the (*Z*)- and (*E*)-isomer, the mixtures of three runs were combined (0.332 g) and carefully chromatographed again (silica gel (400 g); hexane/*t*-BuOMe 4 : 1). A first fraction gave pure (*Z*)-**29** as a brown-red oil (0.138 g). The following fractions delivered enriched (*E*)-**29**, which crystallized after *ca*. 7 d as brown-red needles (0.034 g).

*Data of (*Z*)-***29***:* R_f (hexane/*t*-BuOMe 2 : 1) 0.313. UV/VIS (hexane; see *Fig. 9*): λ_{max} 243 (sh, 4.40), 267 (4.54), 310 (sh, 4.12), 445 (2.77); λ_{min} 219 (4.28), 408 (2.77). IR ($CHCl_3$): 3025*m*, 3015*m*, 2952*w*, 1715v*s*, 1615*w*, 1493v*w*, 1436*s*, 1250v*s*, 1205*w*, 1128v*w*, 1085*m*, 1031*w*, 985v*w*, 937v*w*, 854v*w*, 829v*w*. ^{1}H-NMR (600 MHz, $CDCl_3$): 7.47 (*d*, ^3J = 7.5, H_o of Ph); 7.25 (*s*, H−C(6)); 7.23 (*t*, ^3J = 7.6, H_m of Ph)); 7.12 (*t*, ^3J = 7.3, H_p of Ph)); 6.87 (*s*, H−C(3)); 6.60 (*d*, $^3J(2',1')$ = 12.0, H−C(2′)); 6.35 (*d*, $^3J(12,11)$ = 13.0, H−C(12)); 6.16 (*d*, $^3J(8,9)$ = 5.1, H−C(8)); 6.10 (*d*, $^3J(1',2')$ = 12.0, H−C(1′)); 5.67 (*dd*, $^3J(9,10)$ = 12.4, $^3J(9,8)$ = 5.1, H−C(9)); 5.57 (*dd*, $^3J(10,9)$ = 12.4, $^3J(10,11)$ = 7.6, H−C(10)); 5.51 (*dd*, $^3J(11,12)$ = 13.0, $^3J(11,10)$ = 7.6, H−C(11)); 5.23 (*d*, ^2J = 11.6, H_{syn}−C(13)); 4.86 (*d*, ^2J = 11.6, H_{anti}−C(13)); 3.67 (*s*, MeOCO−C(4)); 3.64 (*s*, MeOCO−C(5)). ^{13}C-NMR (150 MHz, $CDCl_3$): 168.27 (*s*, MeO*C*O−C(5)); 167.79 (*s*, MeO*C*O−C(4)); 146.05 (*d*, C(3)); 144.65 (*d*, C(6)); 144.05 (*s*, C(7)); 139.10 (*s*, C(1)); 138.12 (*d*, C(8)); 136.98 (*s*, C_{ipso} of Ph); 134.18 (*s*, C(2)); 133.33 (*d*, C(2′)); 133.12 (*d*, C(12)); 130.78 (*s*, C(4)); 130.20 (*d*, C(9)); 129.70 (*d*, C(10)); 129.63 (*s*, C(5)); 129.36 (*d*, C(11)); 129.19 (*d*, C_o of Ph); 128.30 (*d*, C_m of Ph); 127.30 (*d*, C_p of Ph); 125.32 (*d*, C(1′)); 52.36 (*q*, *Me*OCO−C(4)); 52.27 (*q*, *Me*OCO−C(5)); 32.84 (*t*, C(13)). GC/MS ($C_{25}H_{22}O_4$; 386.45): 386 (87, M^+), 354 (7), 327 (36, $[M - COOMe]^+$), 326 (22), 311 (11), 295 (39), 294 (15), 268 (42, $[M - 2\ COOMe]^{+\cdot}$), 267 (93), 266 (60), 265 (90), 252 (100), 239 (43), 229 (16), 227 (18), 207 (11), 202 (16), 189 (43), 178 (18), 165 (38), 152 (19), 139 (14), 133 (27), 126 (19), 115 (29), 103 (13), 91 (40), 77 (10).

*Data of (*E*)-***29***:* Brown-red needles. M.p. 188–189° (CH_2Cl_2/Et_2O). R_f (hexane/*t*-BuOMe 2 : 1) 0.291. UV/VIS (hexane; see *Fig. 9*): λ_{max} 235 (4.36), 262 (4.39), 318 (4.61),445 (2.91); λ_{min} 218 (4.21), 244 (4.34), 281 (4.33), 420 (2.91). IR (KBr): 3404v*w*, 3002*w*, 2947*w*, 1711v*s*, 1615*w*, 1495v*w*, 1435*m*, 1310*w*, 1255v*s*, 1159v*w*, 1079*m*, 1067*m*, 1038*w*, 968v*w*, 951*w*, 934*w*, 858v*w*, 784*w*, 754*w*, 723*m*, 693*w*, 659v*w*, 527v*w*. ^{1}H-NMR (600 MHz, $CDCl_3$): 7.45 (*d*, ^3J = 7.5, H_o of Ph); 7.355 (*d*, $^3J(1',2')$ = 15.9, H−C(1′)); 7.346 (*s*, H−C(3)); 7.32 (*t*, ^3J = 7.7, H_m of Ph)); 7.23 (*t*, ^3J = 7.4, H_p of Ph)); 7.20 (*s*, H−C(6)); 6.86 (*d*, $^3J(12,11)$ = 13.2, H−C(12)); 6.61 (*d*, $^3J(2',1')$ = 15.9, H−C(2′)); 6.22 (*d*, $^3J(8,9)$ = 5.0, H−C(8)); 5.85–5.81 (*m*, H−C(9), H−C(11)); 5.77 (*dd*, $^3J(10,9)$ = 12.5, $^3J(10,11)$ = 7.4, H−C(10)); 5.04 (*d*, ^2J = 11.7, H_{syn}−C(13)); 4.65 (*d*, ^2J = 11.7, H_{anti}−C(13)); 3.79 (*s*, MeOCO−C(4)); 3.71 (*s*, MeOCO−C(5)). ^{13}C-NMR (150 MHz, $CDCl_3$): 167.87 (*s*, MeO*C*O−C(5)); 167.31 (*s*, MeO*C*O−C(4)); 145.30 (*s*, C(7)); 144.48 (*d*, C(3)); 143.67 (*d*, C(6)); 138.96 (*s*, C(1)); 138.27 (*d*, C(8)); 137.36 (*s*, C_{ipso} of Ph); 134.11 (*s*, C(2)); 131.53 (*s*, C(5)); 131.10 (*d*, C(12)); 130.20 (*d*, C(11)); 129.79 (*s*, C(4)); 129.51 (*d*, C(10)); 129.34 (*d*, C(2′)); 128.80 (*d*, C(9)); 128.61 (*d*, C_m of Ph); 127.70 (*d*, C_p of Ph); 126.63 (*d*, C_o of Ph); 123.70 (*d*, C(1′)); 52.27 (*q*, *Me*OCO−C(4)); 52.25 (*q*, *Me*OCO−C(5)); 33.31 (*t*, C(13)). GC/MS ($C_{25}H_{22}O_4$; 386.45): 386 (98, $M^{+\cdot}$), 354 (8), 327 (44, $[M - COOMe]^+$), 326 (24), 311 (13), 295 (46), 294 (16), 268 (46, $[M - 2\ COOMe]^{+\cdot}$), 267 (99), 266 (63), 265 (96), 252 (100), 239 (45), 229 (17), 227 (18), 215 (15), 202 (16), 189 (47), 178 (19), 165 (40), 152 (18), 133 (27), 115 (29), 103 (13), 91 (42), 77 (15). Anal. calc. for $C_{25}H_{22}O_4$ (386.45): C 77.70, H 5.74; found: C 77.48, H 5.75.

2.3. *2-[(*Z*)- and (*E*)-2-Phenylethenyl]bicyclo[5.5.1]trideca-1,3,5,7,9,11-hexaene-4,5-dimethanol (=2-[(*Z*)- and (*E*)-2-Phenylethenyl]homoheptalene-4,5-dimethanol*; (*Z*)-**31** and (*E*)-**31**, resp.) *and 2-[(*Z*)-2-Phenylethenyl]-6-oxatricyclo[8.5.1.0^{4,8}]hexadeca-2,4(8),9,11,13,15-hexaen-5-one (=1,3-Dihydro-10-[(*Z*)-2-phenylethenyl]homoheptaleno[4,3-*c*]furan-1-one*; (*Z*)-**32**). Into a soln. of (*Z*)-**29** (0.051 g, 0.132 mmol) in toluene (15 ml) was injected 1.5M DIBAH in toluene (0.105 ml, 0.158 mmol) at −90°. TLC Control after 3 h revealed

still the presence of a large amount of starting material. Therefore, additional DIBAH soln. (*ca.* 0.05 ml, 0.075 mmol) was injected. After a further reduction time of 1 h, all (*Z*)-**29** had reacted, and the soln. was allowed to warm to r.t. Ice-H_2O (10 ml) was added. The toluene phase was washed with 2N aq. HCl soln., H_2O, and sat. NaCl soln., and then dried (Na_2SO_4). CC (silica gel; hexane/*t*-BuOMe 2:1) of the residue of the toluene soln. gave, in a first fraction, (*Z*)-**31** (0.012 g, 28%) as a brown-yellow oil, which, on standing for 1 d in the ice-box, isomerized quantitatively into (*E*)-**31**, and in a second fraction (*Z*)-**32** (0.008 g, 19%) as a violet colored oil, which showed no tendency to undergo (*Z*)/(*E*)-isomerization.

*Data of (*Z*)-***31***: R_f (hexane/*t*-BuOMe 2:1) 0.10. ^{1}H-NMR ($CDCl_3$): 7.51 (*d*, $^3J = 7.2$, H_o of Ph); 7.28 (*t*, $^3J = 7.1$, 2 H_m of Ph)); 7.20 (*t*, $^3J = 7.2$, H_p of Ph)); 6.51, 6.22 (2*d*, *AB*, $^3J_{AB} = 12.0$, H–C(1′,2′)); 6.38 (*d*, $^3J(12,11) = 12.2$, H–C(12)); 6.10 (*s*, H–C(3)); 5.82 (*d*, $^3J(8,9) = 4.9$, H–C(8)); 5.59 (*dd*, $^3J(9,10) = 11.5$, $^3J(9,8) = 5.1$, H–C(9)); 5.53–5.48 (*m*, H–C(6,10,11), 1 H of CH_2(13)); 5.01 (*d*, $^2J = 11.1$, 1 H of CH_2(13)); 4.10 (*d*, *A* of *AB*(1), $^2J_{AB} = 12.5$, CH_2–C(4 or 5); 4.08 (*dd*, *A* of *AB*(2), $^2J_{AB} = 12.5$, $J = 1.1$, CH_2–C(5 or 4)); 3.93 (*d*, *B* of *AB*(2), $^2J_{AB} = 12.5$, CH_2–C(4 or 5)); 3.90 (*d*, *B* of *AB*(2), $^2J_{AB} = 12.5$, CH_2–C(5 or 4)); 1.19 (br. *s*, 2 OH)).

*Data of (*E*)-***31***: Brown-yellow oil. R_f (hexane/*t*-BuOMe 2:1) 0.10. UV/VIS (hexane; see *Fig. 10*): λ_{max} 251 (4.34), 317 (4.43), 326 (sh, 4.39), 362 (sh, 3.64), 430 (sh, 3.20); λ_{min} 220 (4.13), 280 (4.02); tailing up to > 550. IR (film): 3350*m*, 3005*m*, 2956*m*, 2928*m*, 2882*w*, 1597*w*, 1556v*w*, 1492*w*, 1447*m*, 1375*w*, 1303*w*, 1265*m*, 1155v*w*, 1128*w*, 1103*w*, 1055*w*, 1014*s*, 953*m*, 908v*s*, 883*m*, 844*w*, 783*w*, 734v*s*, 695*s*, 668*w*, 648*m*, 552*w*, 519*w*. ^{1}H-NMR (600 MHz, $CDCl_3$): 7.42 (*d*, $^3J = 7.8$, H_o of Ph); 7.40 (*d*, $^3J(1',2') = 16.2$, H–C(1′)); 7.30 (*t*, $^3J = 7.7$, H_m of Ph)); 7.20 (*t*, $^3J = 7.3$, H_p of Ph)); 6.81 (*d*, $^3J(12,11) = 13.1$, H–C(12)); 6.52 (*d*, $^3J(2',1') = 15.9$, H–C(2′)); 6.08 (*s*, H–C(3,6)); 5.87 (*d*, $^3J(8,9) = 5.1$, H–C(8)); 5.78–5.74 (*m*, H–C(9,1)); 5.67 (*dd*, $^3J(10,9) = 12.5$, $^3J(10,11) = 7.5$, H–C(10)); 5.30, 4.64 (2*d*, $^2J = 11.2$, CH_2(13)); 4.47 (*dd*, *A* of *AB*(1), $^2J_{AB} = 12.5$, $J = 1.1$, CH_2–C(4)); 4.31 (*d*, *B* of *AB*(1), $^2J_{AB} = 12.5$, CH_2–C(4)); 4.31, 4.25 (*d*, *AB*(2), $^2J_{AB} = 12.4$, CH_2–C(5)); 2.09 (br. *s*, 2 OH)). ^{13}C-NMR (150 MHz, $CDCl_3$): 147.36 (*s*, C(7)); 141.58, 140.79 (2*s*, C(4,5)); 140.22 (*s*, C(1)); 137.67 (*s*, C_{ipso} of Ph); 135.24 (*d*, C(6)); 135.01 (*s*, C(2)); 133.16 (*d*, C(3)); 133.22 (*d*, C(8)); 130.56 (*d*, C(9)); 130.41 (*d*, C(12)); 128.59 (*d*, C_m of Ph); 128.24 (*d*, C(10)); 127.93 (*d*, C(11)); 127.54 (*d*, C(2′)); 127.37 (*d*, C_p of Ph); 126.46 (*d*, C_o of Ph); 125.08 (*d*, C(1′)); 68.77 (*t*, HO*C*H_2–C(5)); 66.48 (*t*, HO*C*H_2–C(4)); 33.78 (*t*, C(13)).

*Data of (*Z*)-***32***: R_f* (hexane/*t*-BuOMe 2:1) 0.49. UV/VIS (hexane): λ_{max} 261 (4.54); λ_{min} 220 (4.20). IR ($CHCl_3$): 3026*w*, 3016*w*, 1747*s*, 1596*w*, 1449*w*, 1301*w*, 1226*w*, 1135*w*, 1047*w*, 849*w*, 793v*s*, 767*w*, 760v*w*, 722*m*, 696*w*, 672*m*, 667*w*, 463v*w*, 456*w*. ^{1}H-NMR (600 MHz, $CDCl_3$): 7.62 (*d*, $^3J = 7.3$, H_o of Ph); 7.34 (*t*, $^3J = 7.8$, H_m of Ph)); 7.23 (*tt*, $^3J = 7.4$, $^4J = 1.1$, H_p of Ph)); 6.68, 6.31 (2*d*, *AB*, $^2J_{AB} = 11.5$, CH_2–C(16)); 6.47 (*d*, $^3J(2',1') = 11.9$, H–C(2′)); 5.99 (*d*, $^3J(15,14) = 4.9$, H–C(15)); 5.74 (*d*, $^3J(1',2') \approx {}^3J(11,12) \approx 13$, H–C(11,1′)); 5.64 (*s*, H–C(3)); 5.54 (*s*, H–C(9)); 5.47 (*dd*, $^3J(12,11) = 13.0$, $^3J(12,13) = 6.7$, H–C(12)); 5.25 (*dd*, $^3J(14,13) = 12.7$, $^3J(14,15) = 4.9$, H–C(14)); 5.22 (*dd*, $^3J(13,14) = 12.7$, $^3J(13,12) = 6.7$, H–C(13)); 4.43, 4.31 (2*d*, *AB*, $^2J_{AB} = 17.6$, CH_2(7)). ^{13}C-NMR (150 MHz, $CDCl_3$): 173.47 (*s*, O=C(5); 157.13 (*s*, C(8)); 152.53 (*s*, C(10)); 145.60 (*s*, C(2)); 143.73 (*s*, C(1)); 136.53 (*s*, C_{ipso} of Ph); 134.93 (*d*, C(14)); 134.25 (*d*, C(11)); 134.08 (*d*, C(12)); 132.79 (*d*, C(15)); 132.53 (*d*, C(2′)); 131.43 (*d*, C(1′)); 128.84 (*d*, C_o of Ph); 128.49 (*d*, C(13)); 128.23 (*d*, C_m of Ph); 127.35 (*d*, C_p of Ph); 123.39 (*s*, C(4)); 122.24 (*d*, C(3)); 121.75 (*d*, C(9)); 70.33 (*t*, C(7)); 36.12 (*t*, C(16)).

3. X-Ray Crystal-Structure Determinations[10]). – 3.1 *Diacetoxy* **9**. A crystal, obtained from pentane, was mounted on a glass fiber and used for a low-temperature X-ray structure determination. All measurements were made on a *Rigaku AFC5R* diffractometer using graphite-monochromated MoK_α radiation ($\lambda = 0.71069$ Å) and a 12-kW rotating anode generator. The unit-cell constants and an orientation matrix for data collection were obtained from a least-squares refinement of the setting angles of 25 carefully centered reflections in the range $38° < 2\theta < 40°$. The $\omega/2\theta$ scan mode was employed for data collection, where the ω scan width was $(1.21 + 0.35 \cdot \tan\theta)°$ and the ω scan speed was 12° min^{-1}. The weaker reflections [$I < 10\sigma(I)$] were rescanned up to a maximum of 4 scans and the counts were accumulated. Stationary background counts were recorded on each side of the reflection with a peak/background counting-time ratio of 2:1.

The intensities of three standard reflections were measured after every 150 reflections and remained stable throughout the data collection. The intensities were corrected for *Lorentz* and polarization effects. Azimuthal scans of several reflections indicated no need for an absorption correction. The space group was uniquely

---

[10]) Crystallographic data (excluding structure factors) for the structures reported in this paper have been deposited with the *Cambridge Crystallographic Data Center* as supplementary publication Nos. CCDC-159574, 159575, and 159576 for **3**, **9**, and **13**, resp. Copies of the data can be obtained, free of charge, on application to the CCDC, 12 Union Road, Cambridge CB2 1EZ, UK (fax: +44-(0)1223-336033; email: deposit@ccdc.cam.ac.uk).

determined by the systematic absences. Equivalent reflections were merged. Data collection and refinement parameters are given in *Table 8*.

The structure was solved by direct methods with *SHELXS97* [26], which revealed the positions of all non-H-atoms. The non-H-atoms were refined anisotropically. All of the H-atoms were located in a difference electron-density map, and their positions were allowed to refine together with individual isotropic displacement parameters. Refinement of the structure was carried out on F by means full-matrix least-squares procedures, which minimized the function $\Sigma w(|F_o|-|F_c|)$ [26]. The weighting scheme was based on counting statistics and included a factor to down-weight the intense reflections. Plots of $\Sigma w(|F_o|-|F_c|)^2$ *vs.* $|F_o|$, reflection order in data collection, sin θ/λ, and various classes of indices showed no unusual trends. A correction for secondary extinction was applied.

Neutral-atom-scattering factors for non-H-atoms were taken from [27a], and the scattering factors for H-atoms were taken from [28]. Anomalous dispersion effects were included in F_c [29]; the values for f' and f'' were

Table 8. *Crystallographic Data of Compounds* **9**, **3**, *and* **13**

	9	**3**	**13**
Crystallized from	pentane	*t*-BuOMe/hexane	*t*-BuOMe/hexane
Empirical formula	$C_{15}H_{18}O_4$	$C_{17}H_{16}O_4$	$C_{17}H_{16}O_4$
Formula weight [g mol^{-1}]	262.30	284.31	284.31
Crystal color, habit	colorless, prism	red-orange, prism	red, prism
Crystal dimensions [mm]	$0.22\times0.40\times0.50$	$0.27\times0.32\times0.38$	$0.25\times0.30\times0.50$
Temp. [K]	173 (1)	173 (1)	173 (1)
Crystal system	monoclinic	triclinic	monoclinic
Space group	$P2_1/c$	$P\bar{1}$	$P2_1/n$
Z	4	2	4
Reflections for cell determination	25	25	25
2θ range for cell determination [°]	38–40	39–40	34–39
Unit-cell parameters			
a [Å]	8.554 (2)	9.930 (2)	11.891 (2)
b [Å]	12.417 (2)	10.055 (1)	6.997 (4)
c [Å]	12.928 (1)	7.504 (1)	17.072 (2)
α [°]	90	94.88 (1)	90
β [°]	95.67 (1)	109.84 (1)	90.527 (9)
γ [°]	90	82.52 (1)	90
V [Å^3]	1366.4 (4)	698.1 (2)	1420.3 (8)
$F(000)$	560	300	600
D_x [g cm^{-3}]	1.275	1.352	1.329
$\mu(\mathrm{Mo}K_\alpha)$ [mm^{-1}]	0.0917	0.0959	0.0943
Scan type	$\omega/2\theta$	$\omega/2\theta$	$\omega/2\theta$
$2\theta_{(\max)}$ [°]	55	55	55
Total reflections measured	3490	3390	3682
Symmetry independent reflections	3129	3206	3248
R_{int}	0.015	0.017	0.021
Reflections used [$I>\sigma(I)$]	2514	2466	2302
Parameters refined	245	255	255
Reflection/parameter ratio	10.3	9.67	9.03
Final R	0.0397	0.0388	0.0436
wR	0.0379	0.0342	0.0392
Weights: p in $w=[\sigma^2(F_o)+(pF_o)^2]^{-1}$	0.005	0.005	0.005
Goodness of fit	2.009	1.858	1.726
Secondary extinction coefficient	$1.8\,(1)\times10^{-6}$	$2.6\,(3))\times10^{-6}$	$2.9\,(9))\times10^{-7}$
Final Δ_{max}/σ	0.0006	0.0004	0.0006
$\Delta\rho$ (max; min) [e Å^{-3}]	0.23; −0.19	0.23; −0.16	0.22; −0.17
$\sigma(d(\mathrm{C-C}))$ [Å]	0.002	0.002–0.003	0.002–0.003

those from [27b]. The values of the mass attenuation coefficients are those from [27c]. All calculations were performed with the *teXsan* crystallographic software package [30].

3.2. *Homoheptalene-4,5-dicarboxylate* **3**. A crystal, obtained from TBME/hexane, was mounted on a glass fiber and used for a low-temperature X-ray structure determination. All measurements were made on a *Rigaku AFC5R* diffractometer using graphite-monochromated MoK_α radiation ($\lambda = 0.71069$ Å) and a 12-kW rotating-anode generator. The unit-cell constants and an orientation matrix for data collection were obtained from a least-squares refinement of the setting angles of 25 carefully centered reflections in the range $39^\circ < 2\theta < 40^\circ$. The $\omega/2\theta$ scan mode was employed for data collection, where the ω scan width was $(1.52 + 0.35 \cdot \tan\theta)^\circ$ and the ω scan speed was 16° min^{-1}. The weaker reflections [$I < 10\sigma(I)$] were rescanned up to a maximum of 4 scans and the counts were accumulated. Stationary background counts were recorded on each side of the reflection with a peak/background counting-time ratio of 2 : 1.

The intensities of three standard reflections were measured after every 150 reflections and remained stable throughout the data collection. The intensities were corrected for *Lorentz* and polarization effects. Azimuthal scans of several reflections indicated no need for an absorption correction. The space group was determined from packing considerations, a statistical analysis of intensity distribution, and the successful solution and refinement of the structure. Equivalent reflections were merged. Data collection and refinement parameters are given in *Table 8*. The structure was solved by direct methods using *SIR92* [31], which revealed the positions of all non-H-atoms. All further procedures were as described in *Sect. 3.1*. A view of the molecule is shown in the *Fig. 5*. The two seven-membered rings of **3** have quite localized C=C bonds and adopt a *W*-shaped conformation.

3.3. *Homoheptalene-2,3-dicarboxylate* **13**. A crystal obtained from *t*-BuOMe/hexane was mounted on a glass fiber and used for a low-temperature X-ray structure determination. All measurements were made on a *Rigaku AFC5R* diffractometer using graphite-monochromated MoK_α radiation ($\lambda = 0.71069$ Å) and a 12-kW rotating anode generator. The unit cell constants and an orientation matrix for data collection were obtained from a least-squares refinement of the setting angles of 25 carefully centered reflections in the range $34^\circ < 2\theta < 39^\circ$. The $\omega/2\theta$ scan mode was emplyed for data collection, where the ω scan width was $(1.42 + 0.35 \cdot \tan\theta)^\circ$, and the ω scan speed was 16° min^{-1}. The weaker reflections [$I < 10\sigma(I)$] were rescanned up to a maximum of 4 scans and the counts were accumulated. Stationary background counts were recorded on each side of the reflection with a peak/background counting-time ratio of 2 : 1.

The intensities of three standard reflections were measured after every 150 reflections and remained stable throughout the data collection. The intensities were corrected for *Lorentz* and polarization effects. Azimuthal scans of several reflections indicated no need for an absorption correction. The space group was uniquely determined by the systematic absences. Equivalent reflections were merged. Data collection and refinement parameters are given in *Table 8*. The structure was solved as described in *Sect. 3.2*. A view of the molecule is shown in the *Fig. 6*. The two seven-membered rings of **13** have quite localized C=C bonds and adopt again a *W*-shaped conformation.

REFERENCES

[1] E. Vogel, H. Königshofen, J. Wassen, K. Müllen, J. F. M. Oth, *Angew. Chem.* **1974**, *86*, 229; *Angew. Chem., Int. Ed.* **1974**, *13*, 281.

[2] E. Vogel, H. Königshofen, J. Wassen, K. Müllen, J. F. M. Oth, *Angew. Chem.* **1974**, *86*, 777; *Angew. Chem.*, *Int. Ed.* **1974**, *13*, 732.

[3] A. Mugnoli, M. Simonetta, *J. Chem. Soc., Perkin Trans. 2* **1976**, 822.

[4] R. Destro, E. Ortoleva, M. Simonetta, R. Todeschini, *J. Chem. Soc.*, *Perkin Trans. 2* **1983**, 1227.

[5] L. T. Scott, M. A. Kirms, *J. Am. Chem. Soc.* **1982**, *104*, 3530.

[6] L. T. Scott, W. R. Brunsvold, M. A. Kirms, I. Erden, *J. Am. Chem. Soc.* **1981**, *103*, 5216.

[7] L. T. Scott, M. A. Kirms, H. Günther, H. von Puttkamer, *J. Amer. Chem. Soc.* **1983**, *105*, 1372.

[8] A. A. Briquet, P. Uebelhart, H.-J. Hansen, *Helv. Chim. Acta* **1996**, *79*, 2282.

[9] a) S. El Houar, H.-J. Hansen, *Helv. Chim. Acta* **1997**, *80*, 253; S. Maillefer-El Houar, P. Uebelhart, H.-J. Hansen, *Helv. Chim. Acta*, in preparation; b) P. Ott, H.-J. Hansen, *Helv. Chim. Acta* **2001**, *84*, in preparation.

[10] L. T. Scott, C. A. Sumpter, *Org. Synth.* **1993**, *Coll. Vol. VIII*, 196.

[11] E. J. Corey, M. J. Chaykovsky, *J. Am. Chem. Soc.* **1965**, *87*, 1353.

[12] a) S. Moon, *J. Org. Chem.* **1964**, *29*, 3456; b) R. Munday, I. O. Sutherland, *J. Chem. Soc.*, *Chem. Commun.* **1967**, 569; c) R. J. Quellette, D. Miller, A. South Jr., R. D. Robins, *J. Am. Chem. Soc.* **1969**, *91*, 791; d) L. T.

Scott, W. R. Brunsvold, *J. Am. Chem. Soc*. **1978**, *100*, 4320; L. T. Scott, W. R. Brunsvold, M. A. Kirms, I. Erden, *Angew. Chem*. **1981**, *93*, 282; *Angew. Chem.*, *Int. Ed*. **1981**, *20*, XXX; e) P. Kumar, A. T. Rao, K. Saravanan, B. Pandey, *Tetrahedron Lett*. **1995**, *36*, 3397.

[13] H. J. Lindner, B. Kitschke, *Angew. Chem*. **1976**, *88*, 123; *Angew. Chem.*, *Int. Ed*. **1976**, *15*, 106.

[14] Y. Chen, Ph.D. thesis, University of Zurich, 1993.

[15] W. Bernhard, P. Brügger, J. J. Daly, P. Schönholzer, R. H. Weber, H.-J. Hansen, *Helv. Chim. Acta* **1985**, *68*, 415.

[16] A. Linden, M. Meyer, P. Mohler, A. J. Rippert, H.-J. Hansen, *Helv. Chim. Acta* **1999**, *82*, 2274; P. Mohler, A. J. Rippert, H. J. Hansen, *Helv. Chim. Acta* **2000**, *83*, 258.

[17] X. Harada, K. Nakanishi, 'Circular Dichroic Spectroscopy – Exciton Coupling in Organic Chemistry, University Science Books and Oxford University Press, Oxford, 1983.

[18] a) Y. Chen, R. W. Kunz, P. Uebelhart, R. H. Weber, H.-J. Hansen, *Helv. Chim. Acta* **1992**, *75*, 2447; b) R.-A. Fallahpour, H.-J. Hansen, *High Pressure Res.* **1992**, *11*, 125; R. A. Fallahpour, H.-J. Hansen, *Helv. Chim. Acta* **1995**, *78*, 1933.

[19] R. Huisgen, R. Schug, G. Steiner, *Bull. Soc. Chim. Fr*. **1976**, 1813; R. Huisgen, *Acc. Chem. Res.* **1977**, *10*, 117, 199; R. Huisgen, *Pure Appl. Chem*. **1980**, *52*, 2283; and R. Huisgen, *Pure Appl. Chem.* **1981**, *53*, 171.

[20] K. Takahashi, K. Takase, T. Kagawa, *J. Am. Chem. Soc.* **1981**, *103*, 1186.

[21] E. A. Lehto, Ph.D. thesis, University of Zurich, 1997.

[22] P. Brügger, P. Uebelhart, R. W. Kunz, R. Siegrist, H.-J. Hansen, *Helv. Chim. Acta* **1998**, *81*, 2201.

[23] L. T. Scott, C. A. Sumpter, M. Oda, I. Erden, *Tetrahedron Lett*. **1989**, *30*, 305.

[24] A. G. Anderson, R. D. Breazeale, *J. Org. Chem*. **1969**, *34*, 2374.

[25] P. Uebelhart, H.-J. Hansen, *Helv. Chim. Acta* **1992**, *75*, 2493; Y. Chen, H.-J. Hansen, *Helv. Chim. Acta* **1993**, *76*, 168.

[26] G. M. Sheldrick, 'SHELXS97, Program for the Solution of Crystal Structures', University of Göttingen, Germany (1997).

[27] a) E. N. Maslen, A. G. Fox, M. A. O'Keefe, in 'International Tables for Crystallography', Ed. A. J. C. Wilson, Kluwer Academic Publishers, Dordrecht, 1992 Vol. C, Table 6.1.1.1, pp. 477 – 486; b) D. C. Creagh, W. J. McAuley, 'International Tables for Crystallography', Table 4.2.6.8, pp. 219 – 222; c) D. D. Creagh, J. H. Hubbell, 'International Tables for Crystallography', Table 4.2.4.3, pp. 200 – 206.

[28] R. F. Stewart, E. R. Davidson, W. T. Simpson, *J. Chem. Phys.* **1965**, *42*, 3175.

[29] J. A. Ibers, W. C. Hamilton, *Acta Crystallogr.* **1964**, *17*, 781.

[30] *teXsan: Single Crystal Structure Analysis Software*, Version 1.10 pre-release, Molecular Structure Corporation, The Woodlands, Texas, 1999.

[31] A. Altomare, G. Cascarano, C. Giacovazzo, A. Guagliardi, M. C. Burla, G. Polidori, M. Camalli, *SIR92*, *J. Appl. Crystallogr*. **1994**, *27*, 435.

Received January 31, 2001